AD NUMBER

AD803859

NEW LIMITATION CHANGE

TO

Approved for public release, distribution unlimited

FROM

Distribution authorized to U.S. Gov't. agencies and their contractors; Administrative/Operational Use; Nov 1966. Other requests shall be referred to AFWL [WLRP], Kirtland AFB, NM 87117.

AUTHORITY

Air Force Weapons Lab ltr, 30 Nov 1971

AFWL-TR
65-135

STUDY ON SURFACE INITIATION OF EXPLOSIVES

J. Roth

Poulter Research Laboratories
Stanford Research Institute
Menlo Park, California

Contract AF29(601)-6263

TECHNICAL REPORT NO. AFWL-TR-65-135

November 1966

AIR FORCE WEAPONS LABORATORY
Research and Technology Division
Air Force Systems Command
Kirtland Air Force Base
New Mexico

AFWL-TR-65-135

Research and Technology Division
AIR FORCE WEAPONS LABORATORY
Air Force Systems Command
Kirtland Air Force Base
New Mexico

AFWL-TR-65-135

STUDY ON SURFACE INITIATION OF EXPLOSIVES

J. Roth

Poulter Research Laboratories
Stanford Research Institute
Menlo Park, California
Contract AF29(601)-6263

TECHNICAL REPORT NO. AFWL-TR-65-135

FOREWORD

This report was prepared by Stanford Research Institute, Menlo Park, California, under Contract AF29(601)-6263. The research was performed under Program Element 7.60.06.01.D, Project 5710, Subtask 15.018, and was funded by the Defense Atomic Support Agency (DASA).

Inclusive dates of research were 22 October 1963 to 9 April 1965. The report was submitted 26 October 1966 by the AFWL Project Officer, Lt Walter D. Dittmer (WLRP). Former Project Officer on this contract was Lt Richard C. Brightman (WLRP).

The writer gratefully acknowledges the contributions of the following members of Stanford Research Institute: Mr. G. M. Muller for suggesting the "gas flow mechanism" for interpreting the observed front-surface confinement effect and for many helpful discussions of the model of the initiation process; Mr. J. K. Crosby for help in the phases of this study dealing with optics; Mr. F. H. Shipman for assembly and firing of some of the shots and particularly for improving the quality of the shot records; Mr. F. Madlong for assembling and operating the electronic gear; and Mrs. B. Bain for programming and performing all machine computations.

This report has been reviewed and is approved.

Walter D. Dittmer
WALTER D. DITTMER
Lt, USAF
Project Officer

Edgar M. Munyon
EDGAR M. MUNYON
Colonel, USAF
Chief, Physics Branch

Claude K. Stambaugh
CLAUDE K. STAMBAUGH
Colonel, USAF
Chief, Research Division

ABSTRACT

In response to a continued military demand for controlled explosive wave shaping, this study was undertaken to establish basic conditions and to demonstrate the feasibility of an explosive system capable of being initiated uniformly along its entire surface. This investigation is a continuation of those started under AFSWC Contracts AF 29(601)-2844 and -5134. It has demonstrated that under favorable conditions the simultaneity of detonation of a system consisting of surface-confined lead azide sheet, initiated by the radiation from an argon flash-bomb, approaches 0.2 μsec for plane or for hemicylindrical geometry. It is believed that this simultaneity can be improved if techniques for bonding the azide sheet to its confinement are improved. Even without further improvement, the proposed system of surface initiation is capable of providing valuable information in the heretofore experimentally inaccessible region of "simultaneous" loading of curved structures.

CONTENTS

ILLUSTRATIONS

TABLES

This page intentionally left blank.

SECTION I

INTRODUCTION

1. Objectives and Outline of Work

The objective of the work reported here has been to develop the technique for uniform surface initiation of high explosives with pulsed light sources into practical systems of experimental testing value. Initially the program was conceived as a four-part research effort to:

1. Determine the mechanism by which surface confinement increases the reproducibility of initiation delay of PVA lead azide energized by an argon flash-bomb. This included:
   a. Theoretical considerations of motion of product gases and reacting fragments under various geometries.
   b. Study of liquids and flexible solids as confining agents.
   c. Experiments in which confinement was to be varied in a systematic way.
2. Test batches of sheet lead azide under optimum confinement as determined under Item 1.
3. Test performance of the whole system in plane, cylindrical, and spherical geometry. This would cover:
   a. Procedures for handling sensitive explosives remotely.
   b. Measurement of simultaneity of detonation breakthrough on terminal surface with streak camera and pin techniques.
   c. Applications to plate projection and momentum experiments to be made as required by the sponsor.
4. Examine explosives other than lead azide for sensitivity to initiation by light.

2. Degree of Completion

Work on the causes for the surface confinement effect (Item 1 above) is virtually complete. The mechanism proposed explains many heretofore unconnected observations and suggests several methods of improving the reproducibility of initiation delay. Study of Items 2 and 3 was hampered

by the slow and uncertain delivery of sheet lead azide by the sole supplier. As a consequence, no trials have been made on spherical systems, and further experimentation, primarily on improved bonding between the azide sheet and its front-surface confinement, is necessary for cylindrical systems. No other explosives (Item 4) suitable for surface initiation by light have been found.

3. Previous Work

The primary objective of the previous investigations[1,2] was to determine which factors influence the variability in metal azide initiation delay for systems energized by argon flash-bombs. To achieve a practical surface initiation system, this variability must be kept small.

The main findings of these investigations may be summarized as follows:

1. Ball-milled PVA lead azide shows less initiation delay variability (jitter) than silver azide which, in turn, has much less jitter than dextrinated lead azide.
2. Jitter is reduced by placing glass, quartz, or plastic "windows" in close contact with the azide surface facing the flash-bomb.
3. Usually jitter is a fairly constant fraction of the initiation delay. To reduce absolute jitter, initiation delays should be kept small.
4. The argon flash-bomb is a blackbody radiator at 29,000° K.
5. Quantitative methods of obtaining the radiation divergence loss for flash-bombs and correcting for the finite rise time to peak radiation intensity were developed.
6. The initiation delay is inversely proportional to the rate of energy absorption of the irradiated surface.
7. The lead azide initiation process is thermal rather than photochemical.
8. The kinetic parameters obtainable on the basis of the above agree well with those obtained by others for lead azide decomposition without explosion.
9. A continuous lead azide surface, e.g., lead azide sheet, is easier to use and is capable of providing less jitter than multipoint initiation by many closely spaced lead azide assemblies.

SECTION II

EXPERIMENTAL WORK

1. General Considerations

The main objective of this study was the development of a practical system of surface initiation. The system under investigation consists of lead azide as the initiating explosive and the radiation from an argon flash-bomb as the energy source. To achieve the objective, the jitter in the lead azide initiation delay must be small. Many factors could influence the initiation delay and delay jitter. The most obvious are the amount and spectral region of the absorbed argon radiation. Other factors might be particle size, purity, packing density, and prior conditioning of the azide. Confinement of the azide layers that absorb radiation might also be important. Finally, to develop a practical system, an explosive train having no more jitter than the azide initiation must be designed and tested.

For a better understanding of the experiments to be described, an idealized schematic presentation of the system investigated is shown in figure 1. To study the effects of absorbed energy on initiation delay and delay jitter, one must know the energy incident on the azide and determine what fraction of this energy is absorbed. This requires a knowledge of all the parameters listed in figure 1. The effects of confinement may be studied by changing the position and type of window. Prior conditioning of the azide presumably affects α_λ and R_λ.

Initiation delays can be conveniently determined by viewing with a streak camera the azide face opposite that which absorbs the radiation and correcting for the transit time of an established detonation through the azide assembly. Thus measurements of azide transit times have to be made for various loading densities, purity, and particle sizes.

2. Procedures and Apparatus

Procedures for loading, positioning, and obtaining streak camera

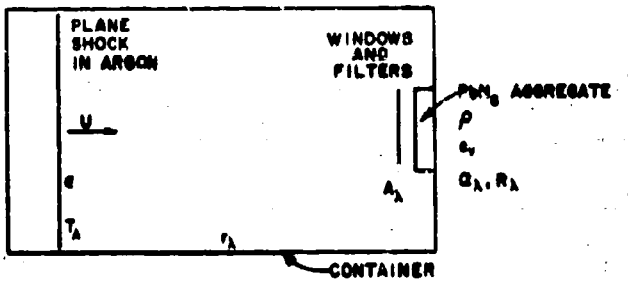

U • SHOCK VELOCITY

ϵ • EMISSIVITY OF SHOCKED ARGON

T_λ • TEMPERATURE OF SHOCKED ARGON

r_λ • REFLECTIVITY OF CONTAINER WALLS

A_λ • TRANSMISSIVITY OF WINDOWS AND FILTERS

ρ • PACKING DENSITY OF AZIDE

c_v • SPECIFIC HEAT OF AZIDE

α_λ • RADIATION ABSORPTION COEFFICIENT OF AZIDE

R_λ • RADIATION REFLECTION COEFFICIENT OF AZIDE

Figure 1 SCHEMATIC DIAGRAM OF LEAD AZIDE — FLASH-BOMB SYSTEM

records of the initiation of granular lead azide assemblies have been described in detail in the Experimental Section of Ref. 2. The "standard" assembly consists of a nylon sleeve 0.500 inch OD, 0.188 inch ID, 0.100 inch high, with a glass window attached to an empty sleeve and packed with ball-milled PVA lead azide to around 2.3 to 2.4 g/cc. Also described in Ref. 2 are the filters used for varying the energy delivered to the azide by the argon flash-bomb, and the monitoring of this energy by a specially designed photomultiplier system. All this remains unchanged in the present investigation. New techniques for handling sheet azide are given in the following section.

Transit times for an established detonation to move through an azide assembly were previously obtained by pin techniques.[2] These often gave erratic results. Since it has been established[1, 2] that initiation occurs very near the irradiated surface, and under controlled conditions delay jitter is very small, transit times are now obtained by measuring, in the same shot, the total delay (initiation delay plus transit time) of several identical assemblies of different azide thickness and obtaining the transit time by difference. Transit time results, in the form of a detonation velocity vs packing density plot, are summarized in figure 2.

In studying the effect of confinement some new "windows" have been used. Their transmissivity is shown in figures 3(a) and 3(b).

2. Handling of sheet azide

This material is received kerosene-wet in roughly 3 x 3 x 0.03 inch sheets. The physical properties of sheet azide made by the Dupont Company are given in Table 1. While still wet, it is placed on lead sheets (behind an armor glass shield) and cut into 1.5-inch squares and short thin strips using razor blades mounted on long handles. The strips are then cut into approximately 1/4-inch-diameter disks using a freshly sharpened cork-borer mounted so that the cutting can be done remotely. The squares and disks are then flushed with petroleum ether and air dried. To prevent

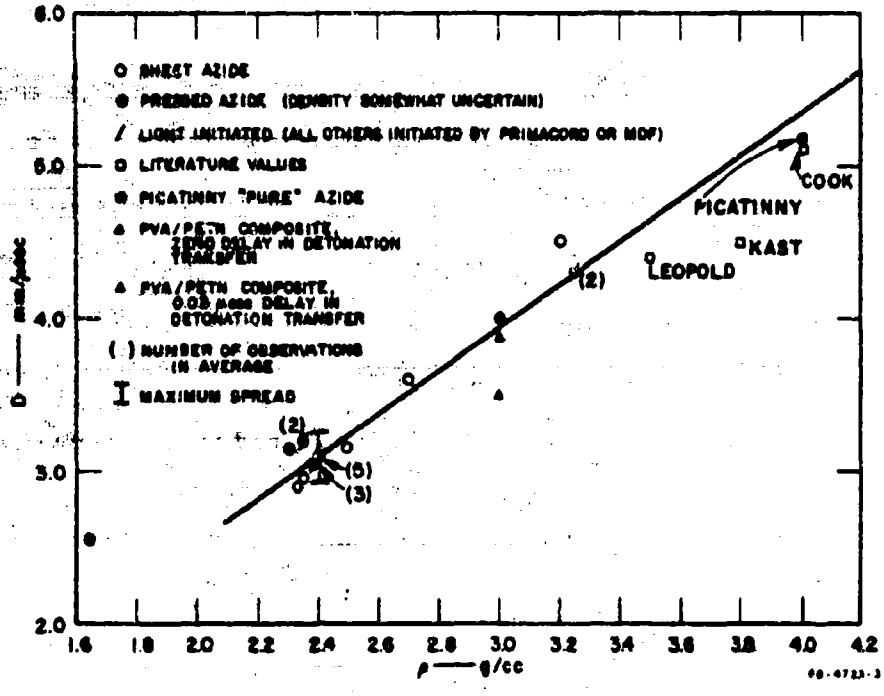

Figure 2 DETONATION VELOCITY OF LEAD AZIDE

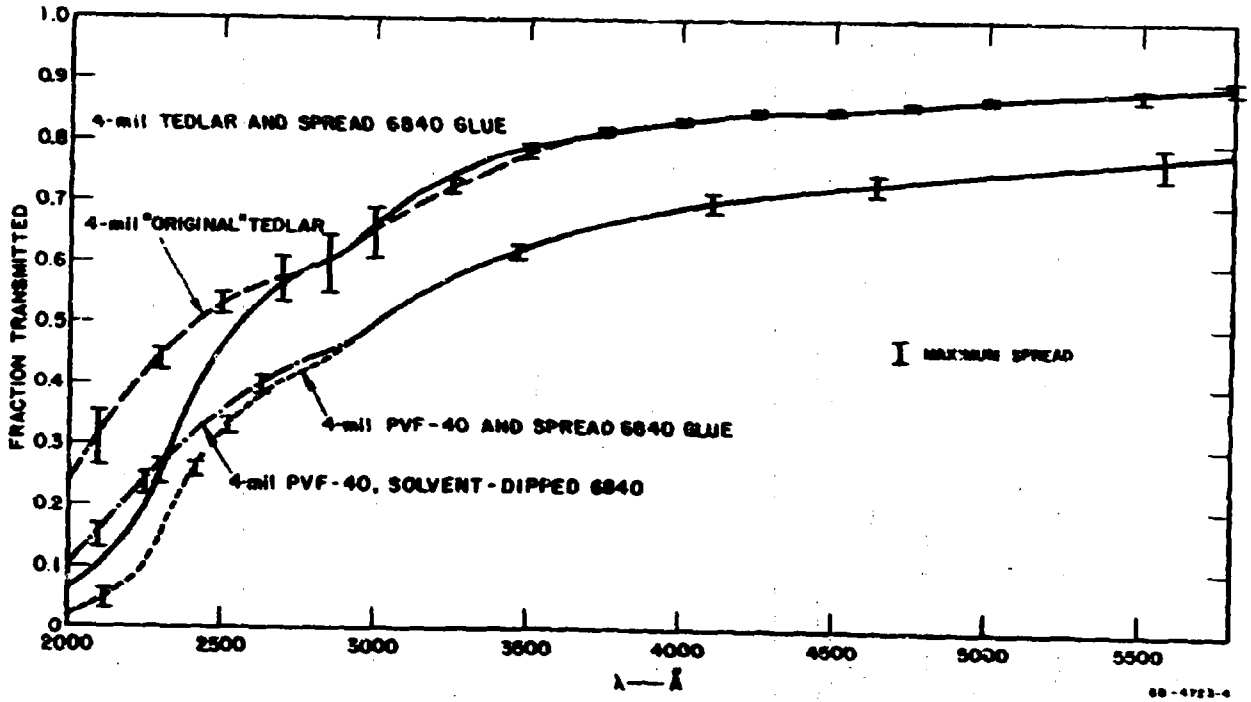

Figure 3(a) TRANSMISSIVITIES OF PLASTIC "WINDOWS"

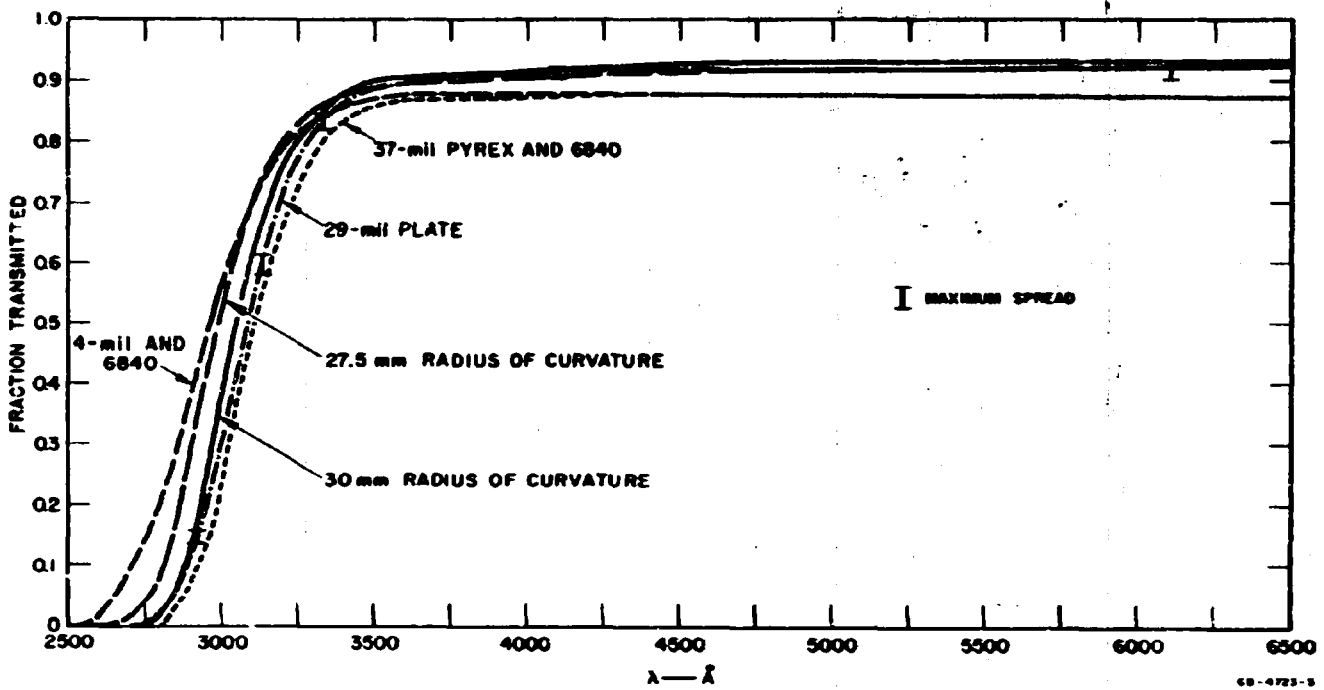

Figure 3(b) TRANSMISSIVITIES OF GLASS "WINDOWS"

Table 1

PROPERTIES OF LEAD AZIDE AND PETN SHEET

Batch No.	Composition	Average Thickness (mils)	Density as Received (g/cc)
1	95/5 RD 1333 Azide/Teflon	30	2.2
2		36	?
3		37	2.7
4		23	?
5		33	2.5
6	95/5 Colloidal Azide/Teflon	24	2.5
7		26	2.6
8	95/5 RD 1333 Azide/Teflon	34	2.5-2.6
9		31	2.6
10		36	2.5
11		27	2.6
12		22	2.8
13		28	2.6
1st shipment	90/10 PETN/Teflon	31	1.3
2nd shipment		27	1.3

generation of dangerous electrostatic charges, all metal objects in the room where these operations occur are grounded. The room has a conductive floor and the operator wears conductive rubber or leather-soled shoes.

b. Shot assembly

Sheet azide was used as disks for control assemblies and as 1.5-inch squares for surface initiation experiments. The sheet azide squares were almost always a part of an explosive train which at its simplest contained sheet azide and 90/10 PETN/Teflon binder sheet ($\rho \sim 1.3$ g/cc). Some trains had these sheets placed over EL-506D or EL-506D mounted on slabs of Comp B. Good photographic records were obtained with the systems containing Comp B (always 0.500 inch thick). The sheet azide and sheet PETN, however, are sufficiently translucent to have the tremendous light flux of the argon flash-bomb fog the film even at streak camera mirror speeds of 2000 rps. To prevent this, two or three coats of glossy black lacquer must be placed on the PETN sheet surface facing the camera. The best records were obtained if, in addition to the lacquering, the sheets were attached to lenticular plastics so that the air and/or argon trapped between the explosive and the plastic became highly luminous when hit by the detonation shock of the explosive sheet. Bagley[3] has shown that this luminosity is achieved in a few nanoseconds. A shot holder for flexible explosives is shown in figure 4. The main charge in this shot was a section of a cylinder. For plane geometry shots, a square of lenticular plastic was used rather than the curved plastic shown in figure 4. The circular holes are for controls which enable one to relate any given shot to previous shots. Of the six controls in this arrangement, at least two are "standard" granular lead azide assemblies. These are mounted directly into the circular holes. For sheet azide controls, optimum records were obtained when these were mounted on disks of lenticular plastic (not shown in figure 4). Assembly of explosives in the shot holder to the argon flash-bomb was the same as that given in Ref. 2.

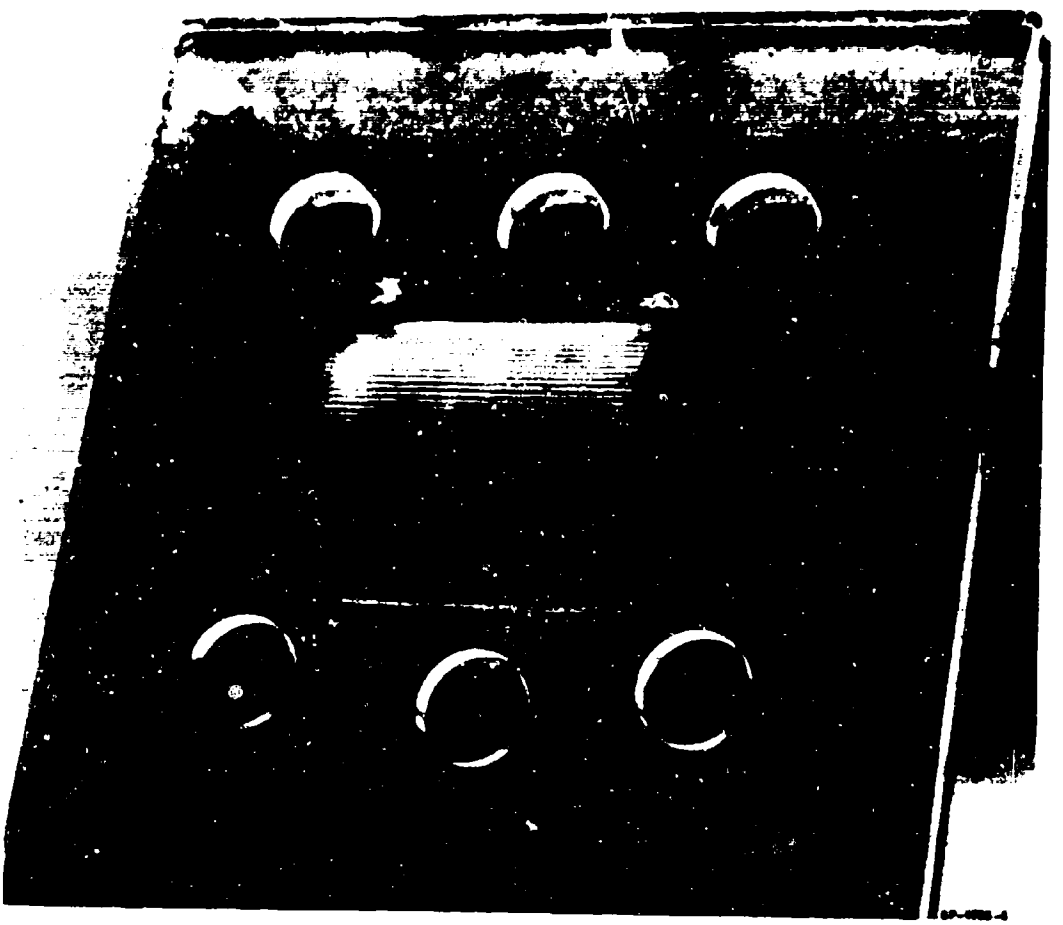

Figure 4 HOLDER FOR HEMICYLINDRICAL SHOTS

The shots using Comp B slabs were prepared differently from ones above because they contained more explosive and because they came at a time when we had relatively little experience in handling sheet azide. As shown in figure 5 and the engineering drawings (figure 6), the shot holder was made in two parts. One part contained the Comp B slab, the EL-506D, and the PETN sheet. The other part contained the lead azide sheet with its surface confinement. These parts were kept separate until the shot was almost ready for shooting. Note the tapped holes in the plastic (figure 5) which were used for bringing the test explosive to the argon box by means of a long rod with a threaded inner rod. As shown, the lead azide sheet holder was held to the argon box by magnets and the rest of the explosive was positioned against the lead azide sheet by another magnet. This arrangement had the usual provisions for mounting control assemblies.

c. Surface confinement

As will be shown later, surface confinement has a profound influence on delay jitter. Providing adequately uniform confinement is rather simple for standard granular azide assemblies. The confinement is attached to an empty sleeve which is then press-loaded with lead azide.[2] Because of its flexible nature and because its binder--Teflon--(which congregates on the surface) is notoriously hard to bond to anything, the above scheme does not work well with sheet azide. A completely foolproof scheme of attaching confinement to sheet azide remains to be devised. A technique which works most of the time is as follows: a thin layer of Dupont 6840 acrylic-base glue is spread as uniformly as possible over the azide surface. This glue is very transparent all the way down to 2400 Å. Azide disks for controls are placed on the confining medium (glass or plastic disks) and pressed in a cylindrical die to around 2000-3000 psi. In testing the quality of the bond between the confinement and sheet azide it was found that usually, but not always, the confinement could be pulled off with a thin layer of sheet azide attached to it, indicating fairly good bonding. For plane geometry, as well as some hemicylindrical assemblies, glue-covered confinement was

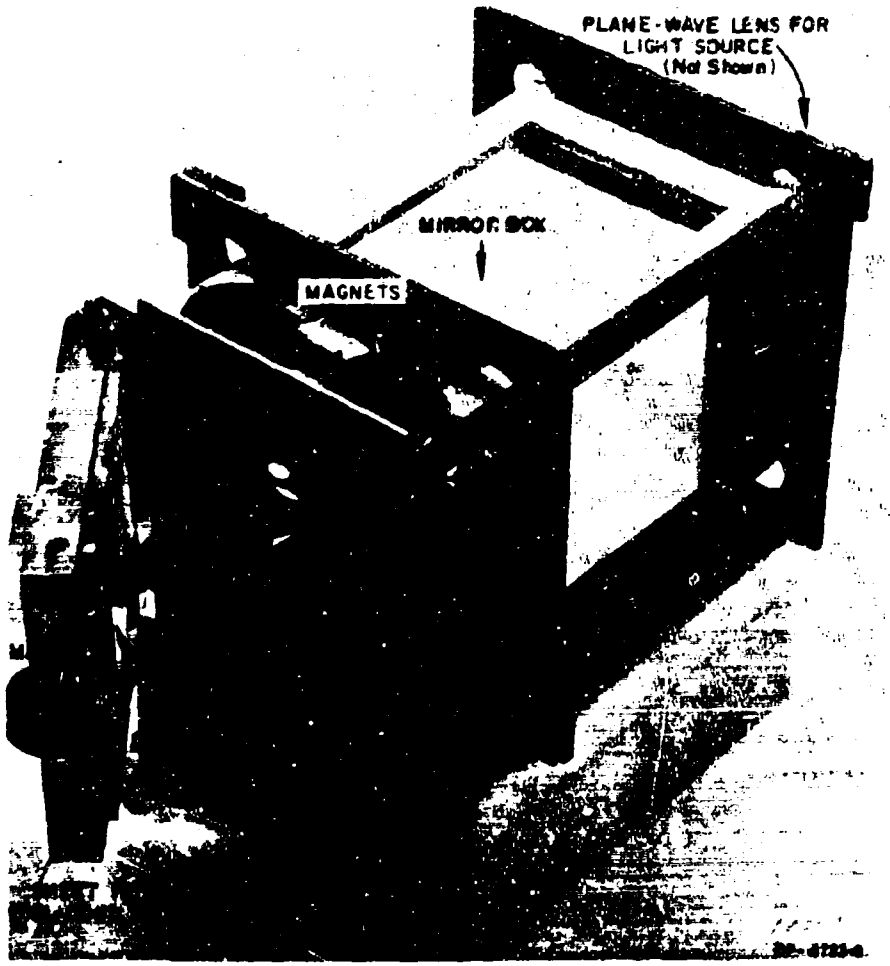

Figure 5 SHOT ASSEMBLY FOR PLANE-WAVE SHOTS

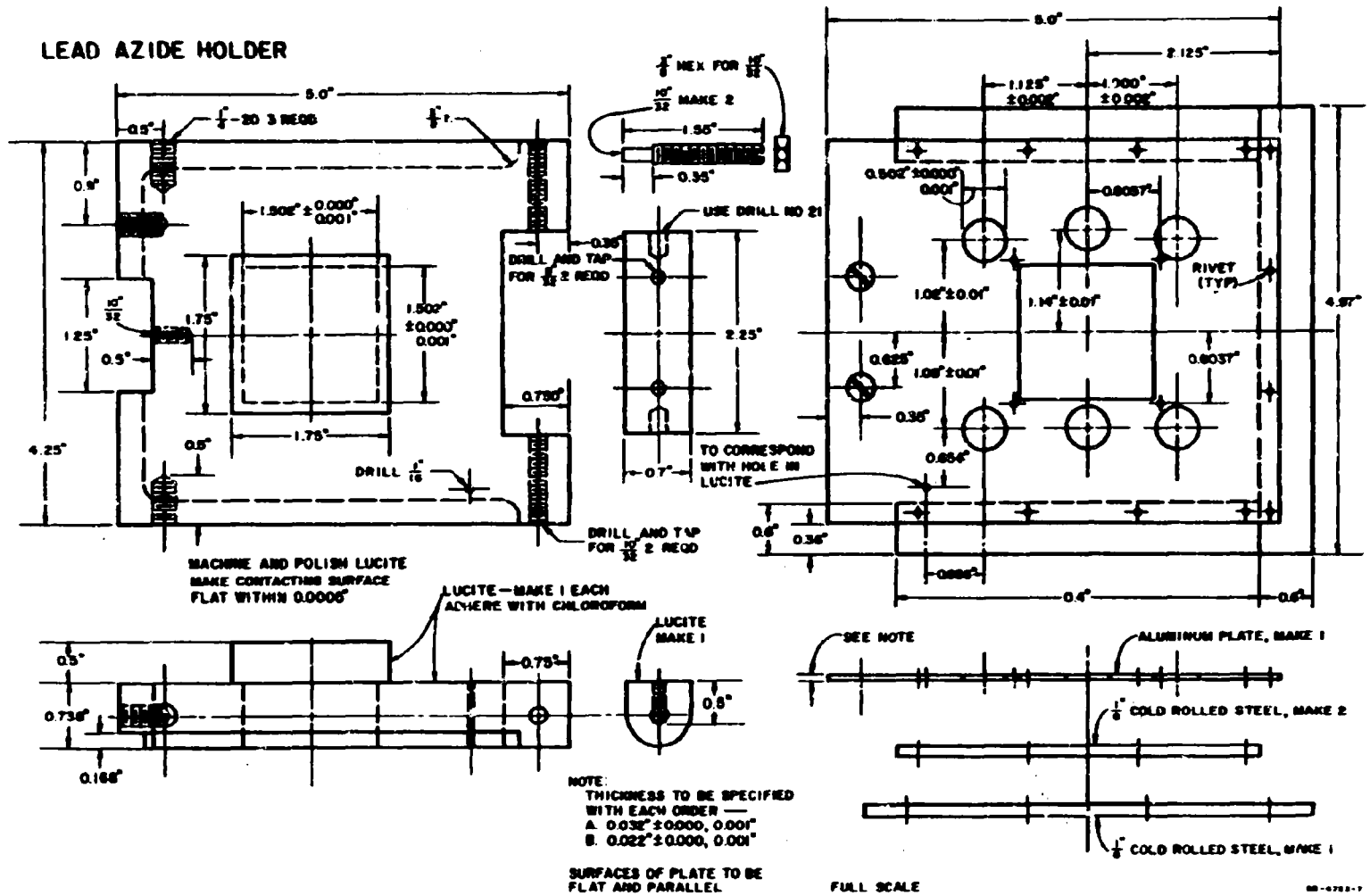

Figure 6 LEAD AZIDE HOLDER FOR PLANE-WAVE SHOTS

pressed against the sheet azide, contained in a die having the same cross section and height as the azide sheet, at around 3000-5000 psi. In making these flat pressings conform to a curved surface (e.g., as in figure 4), some separation between confinement and sheet azide often occurred. To circumvent this, some pressings were made against curved glass confinement supported by a Cerrobend (an alloy melting in boiling water) mold. Although the bond between sheet and confinement appeared to be good, the glass confinement was cracked in most pressings. This increased jitter, as will be shown later.

d. High-density pressings

In determining the causes responsible for the surface confinement effect it became important to measure the initiation delay for highly compressed lead azide, both granular and sheet. Cylindrical hardened tool steel dies were used in the range of 1×10^5 to 2×10^5 psi. The highest densities achieved were about 4.4 g/cc for granular lead azide and 4.1 g/cc for sheet lead azide. These are, respectively, about 92 and 90% of voidless density. The granular azide was pressed into mild steel sleeves which were allowed to expand laterally in order to prevent azide "spring-back." Successive pressings at progressively lower pressures were found to be very helpful.

e. Raised window effect

It has been shown[2] that moving the front-surface confinement "windows" by as little as 1 mil away from the irradiated azide face causes an appreciable increase in the initiation delay. These phenomena have been examined further, particularly in having the space between azide and window evacuated or filled by compressed nitrogen. Some trials were also made with windows raised above high-density azide pressings. The vacuum trials were made as follows: A hypodermic needle was cemented in a groove starting at the shot-holder positioning hole and running along the shot-holder surface (similar to the one shown in figure 4). A standard azide assembly without a window was placed in the positioning hole, and a window was

cemented to the shot holder over the positioning hole and over most of the groove for the hypodermic needle. Using a diffusion pump, the approximately 20- to 25-mil-thick air space above the azide could be evacuated to below 10μ Hg. An entirely analogous arrangement which was not evacuated served as control. The pressurized systems consisted of a standard, windowless, azide assembly contained between two pieces of thick glass held together by a metal frame-gasket-and-bolt arrangement, and provided with a high-pressure tubing inlet. Using a high-pressure nitrogen cylinder, the approximately 100-mil space above the azide was pressurized to 21 atmospheres. Controls were exactly as described above but at ambient air pressure.

f. Light intensity

As has been shown,[2] photomultiplier records of peak relative intensity of the argon flash and of the time to reach this peak are important in understanding the shot-to-shot variation of initiation delay. Measurement of absolute intensity leads to a fundamental understanding of the initiation mechanism, because it permits the establishment of a relation between the observed initiation delay and the energy absorbed by the azide.[2] Two new schemes were tried to improve the reliability of the measurement of absolute intensity--more properly speaking, the temperature of the argon flash. A photo-tube of the same spectral response as before but of higher output enabled us to use a rotating sector in front of the standard tungsten ribbon source.[2] Thus an easier-to-read square-wave signal was obtained rather than the dc shift previously recorded.[2] Several seemingly straightforward theoretical calculations of the temperature of shocked nitrogen are available.[4, 5] Since these are much closer to the argon temperature than the tungsten ribbon temperature, their use as "standards" should greatly reduce calibration uncertainty. Comparisons between argon and nitrogen, in the usual flash-bomb system, were made at 5000 Å, 4500 Å, and 4000 Å. The results of these new calibrations will be presented in Section II-3b.

g. Attempts to initiate nitroglycerin and PETN

In the present system of surface initiation it would be desirable to use initiating explosives less sensitive than lead azide. Particularly attractive would be a liquid explosive because it would conform to any desired surface. With this in mind, attempts (which were unsuccessful) were made to initiate nitroglycerin or PETN using the usual argon flash-bomb system. About 0.1% of Nigrosine (a black organic dye) was dissolved in the nitroglycerin to make it more radiation-absorbent. It was determined subsequently that more Nigrosine should have been used, but the initial experiments were sufficiently discouraging that no further trials were made. Blackened nitroglycerin was introduced with a hypodermic needle through a small hole in the sidewall into a cylindrical container with flat quartz windows. This assembly was positioned and attached to the flash-bomb in the usual manner. Subsieve particle size PETN, pure or dry-mixed with very fine graphite, was press-loaded into "standard" sleeves with windows attached to the empty sleeves. In a few instances these pressings were done in two increments to obtain regions of different packing density. Results are given in Section II-3h.

3. Results

a. Effective light intensity

As defined previously,[2] the effective light intensity $\bar{I}$ is given by

$$\bar{I} = \frac{\int_0^T I_{rel}(t)dt}{T} \qquad (1)$$

where I_{rel} is obtained directly from a photomultiplier record. $\bar{I}$ is also a function of the wavelength of light at which I_{rel} is obtained. Figure 7 gives the latest $\bar{I}$ vs t curves. These results are replotted in figure 8 as $\bar{I}$ vs wavelength viewed by the photomultiplier. It is obvious from figure 8 that the variation of $\bar{I}$ with λ for $\lambda < 3000$ Å is highly speculative since there are no experimental determinations in this region.

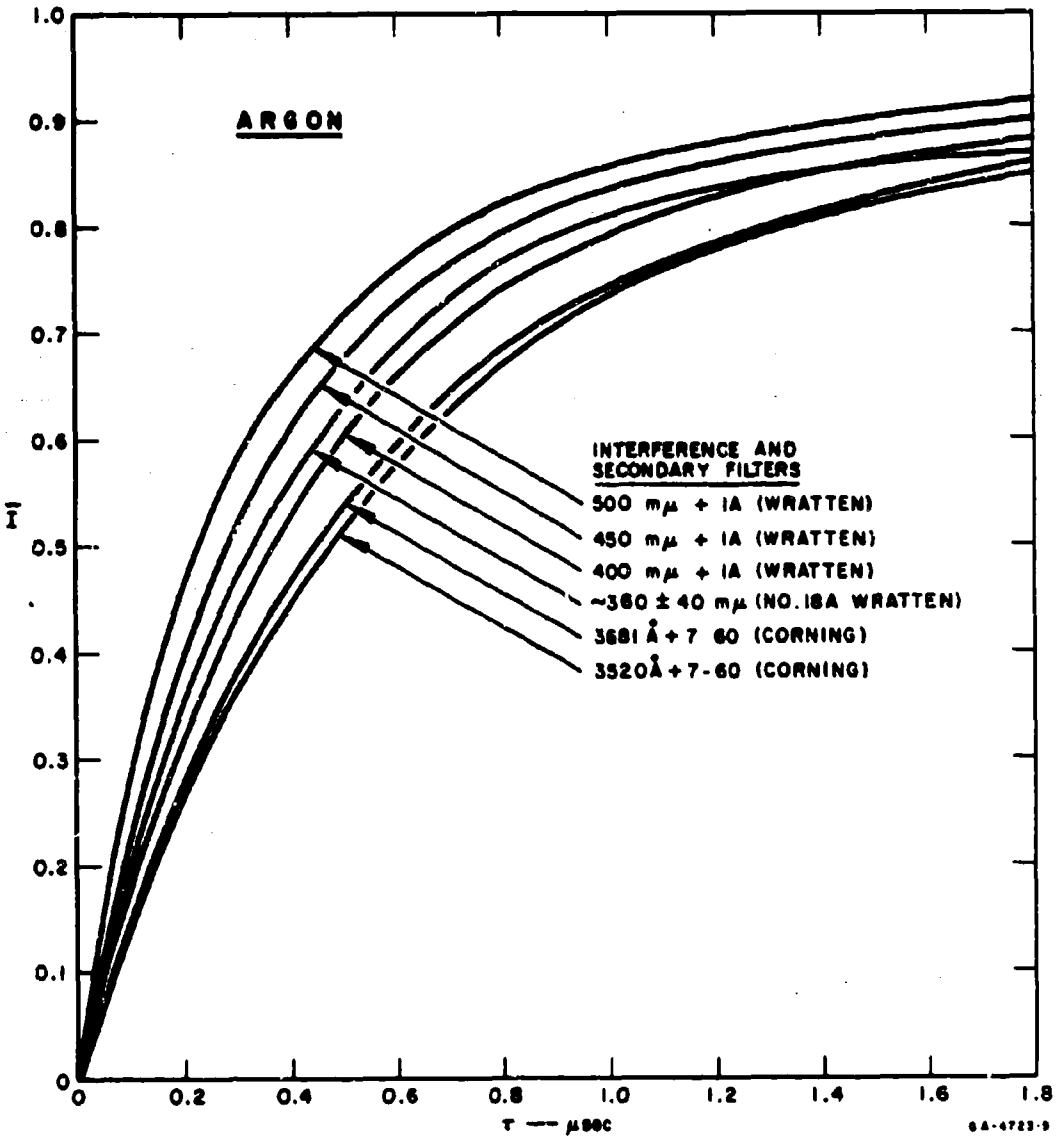

Figure 7 EFFECTIVE LIGHT INTENSITY vs. TIME FOR ARGON (See Eq. 1)

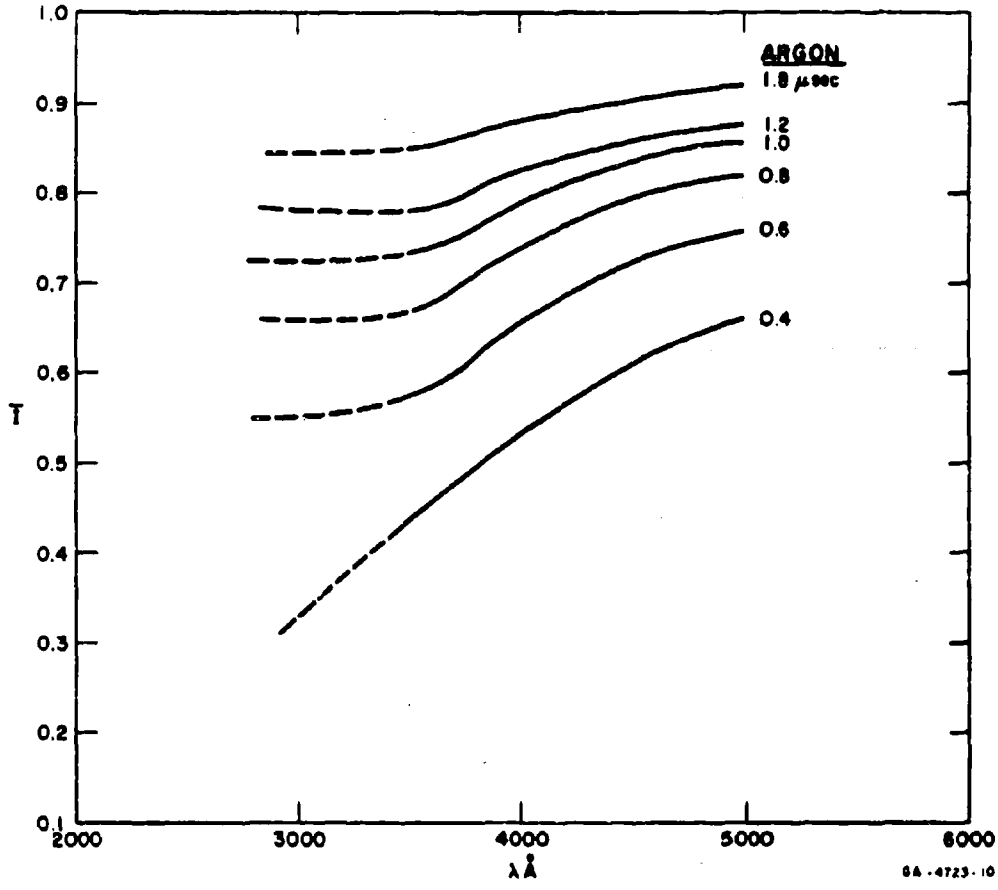

Figure 8 EFFECTIVE LIGHT INTENSITY vs. WAVELENGTH FOR ARGON

Figure 9 shows $\bar{I}$ vs t curves for nitrogen flash-bombs. Note the much longer time required to reach the "flat" portions of these curves.

b. Temperature measurements of shocked argon

Using the photomultiplier-interference filter system and the electronic xenon flash as internal calibration (described previously[2]), comparisons were obtained between argon flashes and a standard tungsten ribbon source or nitrogen flash-bombs. In the tungsten source comparisons (see Sec. II-2f) "small-scale shots" described in Refs. 2 and 6 were used. The comparison between argon and nitrogen flashes was made in the usual mirror-box systems. In both cases the argon temperature is obtained from a solution[2, 6] of the following equations for different radiators in the same optical system [Eq. (2)], and the same radiator in different optical systems [Eq. (3)]:

$$H_A/H_S = \int_{\lambda_1}^{\lambda_2} \epsilon_A(\lambda)N_A(\lambda, T_A)A(\lambda)P(\lambda)d\lambda \Big/ \int_{\lambda_1}^{\lambda_2} \epsilon_s(\lambda)N_s(\lambda, T_s)A(\lambda)P(\lambda)d\lambda \qquad (2)$$

$$H_1/H_2 = \int_{\lambda_1}^{\lambda_2} \epsilon_1(\lambda)N_1(\lambda, T)A_1(\lambda)P_1(\lambda)d\lambda \Big/ \int_{\lambda_3}^{\lambda_4} \epsilon_2(\lambda)N_2(\lambda, T)A_2(\lambda)P_2(\lambda)d\lambda \qquad (3)$$

The subscript "A" refers to argon and "s" to the standard. Here H is the observed photomultiplier output, ϵ is the radiator emissivity, N is its blackbody function, A is the transmissivity of all windows and filters in the light path (for the mirror box shots it also includes the wavelength-dependent reflectivity of a standard paper reflector used in the optical path), and P is the spectral response of the photomultiplier. The integration limits are determined by the particular interference filter used. The ratio of H's is usually referred to as H_{rel}.

The color temperature of the tungsten ribbon was rechecked using pyrometers. These measurements ranged between 2360 and 2380° K, generally clustering more around the higher value. As shown in Table 2,

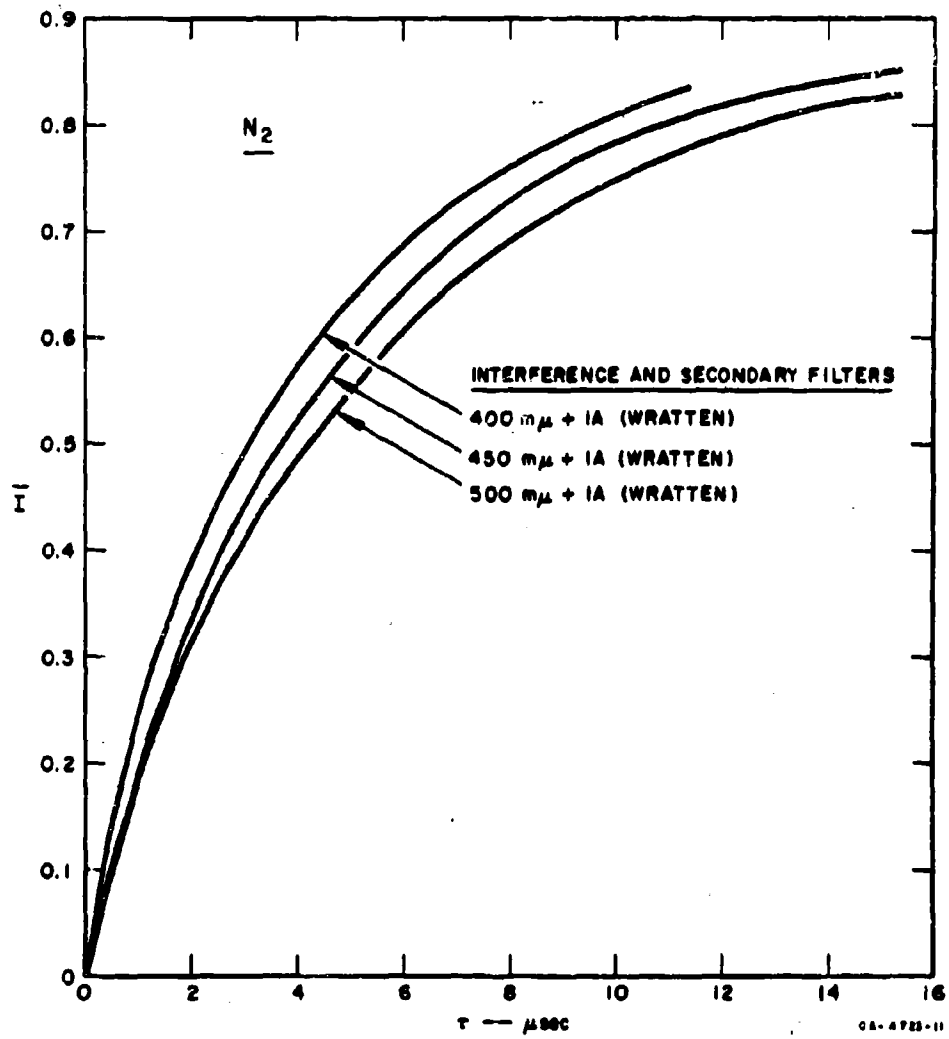

Figure 9 EFFECTIVE LIGHT INTENSITY vs. TIME FOR N_2

Table 2

TEMPERATURE OF TUNGSTEN RIBBON SOURCE

Filters*	$\int NAP d\lambda = B^{**}$ (watts/cm^2/steradian)	B_{rel}**	$B_{rel}\epsilon_{rel}$			H_{rel}***
			$T_s = 2380^\circ K$	$2370^\circ K$	$2340^\circ K$	
600 + No. 8	10.27×10^{-3}(a)	2.42(a)	2.32(a)	2.35(a)	2.45(a)	2.52
500 + 1A	10.05×10^{-3}	2.36	2.35	2.37	2.40	2.40
450 + 1A	4.25×10^{-3}	1.000	1.000	1.000	1.000	1.000
400 + 1A	1.50×10^{-3}	0.353	0.358	0.356	0.347	0.356
368.1 + 7-60	0.278×10^{-3}	0.0655	0.067	0.066	0.063	0.066
18A	1.23×10^{-3}(a)	0.290	0.290(a)	0.285(a)	0.277(a)	0.288

* First number is peak transmission wavelength in mμ; second number is auxiliary filter designation.

** For $T_s = 2380^\circ$ K.

*** H_{rel} = photomultiplier output for a given filter divided by the photomultiplier output at 450 mμ + 1A.

(a) Somewhat uncertain because of uncertainties in P in this spectral region.

experimental results of photomultiplier measurements (H_1/H_2) analyzed by Eq. (3) lead to a source temperature of 2370 to 2380° K. Using observed H_A/H_S in Eq. (2) and taking T_s = 2370° K or 2380° K, gives T_A = 28,000° K or T_A = 29,000° K, respectively, as shown in Table 3. The comparisons [Eq. (2)] between argon and nitrogen are given in Table 4. For the observed N_2 shock velocity of 8.1 mm/μsec, theoretical calculations of Christian et al.[4] give T_{N_2} = 11,000° K and those of Thouvenin[5] give T_{N_2} = 11,200° K. Thus the results in Tables 3 and 4 strongly support the view that T_A lies between 28,000 and 29,000° K. Moreover, these results confirm our belief[2,6] that the argon flash is a blackbody radiator. The nitrogen flash also appears to be blackbody.

c. Initiation delays of granular lead azide

All the initiation delays for granular lead azide measured during this investigation and the conditions of measurement are listed in Table 5. As discussed previously,[2] sun tanning of the azide appears to reduce initiation delay jitter. Therefore, all assemblies were exposed to noon sunlight ("sun tanned") for four minutes on the day before the shot. Exposure was through the window of an assembly. Filters, if used, were placed over the windows after sun tanning. Normalization of all delays to enable shot-to-shot comparison was the same as used previously.[2]

It was established that the increase in initiation delay with increasing azide packing density is not, as suspected previously,[2] a spurious effect due to the decrease in azide column diameter for the high-density pressings. Recent loadings (see Sec. II-2d) show quite conclusively that this density effect is independent of column diameter (see figure 10).

d. Initiation delays for sheet lead azide

In all surface initiation trials approximately 1/4-inch-diameter sheet azide disks were used as controls. Normalized initiation delays for front-surface confined disks of all sheet azide batches, except 1 and 2 which were shot before a reliable method of attaching confinement was

Table 3

TEMPERATURE OF COMP B GENERATED SHOCK IN ARGON

(Tungsten Ribbon Standard--"Small-Scale" Shots)

Filters*	H_A/H_S		$\int N_A A P d\lambda$ = B**	$\int N_S A P d\lambda$ = C**	$B/\epsilon_s C$***	
	Average	Range	(watts/cm^2/steradian)			
600 + No. 8	102	99- 105(b)	0.496	10.27×10^{-3}	104	102(a)
500 + 1A	416	402- 431	1.915	10.05×10^{-3}	421	417(a)
450 + 1A	918	890- 930(b)	1.822	4.25×10^{-3}	935	925(a)
400 + 1A	1125	1110-1140	0.808	1.50×10^{-3}	1160	1150(a)
368.1 + 7-60	4770	4750-4790	0.621	0.278×10^{-3}	4770	4760(a)

* First number is peak transmission wavelength in mμ; second number is auxiliary filter designation.

** See Eq. (2), $T_A = 29,000°K$; $T_S = 2380°K$. For all shots A includes N.D. filters.

*** ϵ_s from Ref. 6; $\epsilon_A = 1.00$.

(a) $T_A = 28,000°K$; $T_S = 2370°K$.

(b) Three measurements; all others two measurements.

Table 4

COMPARISON OF ARGON AND NITROGEN FLASH-BOMBS

(Comp B Generated Shock in Standard Mirror Bombs)

Filters*	$\frac{\text{Peak Shot Intensity}}{\text{Peak Flasher Intensity}} = M$	Normalization Factor** = N	H = MN	$\int NAPd\lambda = C$ Arbitrary Units***	H_{rel}	C_{rel}		
ARGON								
600 + No. 8	0.925	1.04	0.962	1.68	0.151	0.143(a)		
	0.778	1.22	0.950	1.68	0.149	1.143(a)		
	0.950	1.00	0.950	1.68	0.149	0.143(a)		
500 + 1A	4.55	1.15	5.24	9.56	0.824	0.819(a)		
	5.10	1.03	5.25	9.56	0.825	0.819(a)		
450 + 1A	5.95	1.10	6.54	11.68	-	-		
	6.06	1.04	6.30	11.68	-	-		
	6.00	1.00	6.25	11.68	-	-		
			Avg 6.36	11.68	1.000	1.000(a)		
400 + 1A	4.30(b)	1.20	5.15	10.16	0.809(b)	0.873(a)		
	4.88(b)	?	-	10.16	-	0.873(a)		
	4.50(b)	1.15	5.18	10.16	0.815(b)	0.873(a)		
	5.16(b)	1.01	5.20	10.16	0.817(b)	0.873(a)		
368.1 + 7-60	1.88(a)	1.01	1.90	4.21	0.298(b)	0.362(a)		
	1.88(a)	1.05	1.90	4.21	0.310(b)	0.362(a)		
NITROGEN								
500 + 1A	0.715	1.00	0.715	1.305	7.35	7.33	7.39(c)	7.35(d)
450 + 1A	0.770	~1.0	~0.770	1.420	~8.26	8.23	8.30(c)	8.30(d)
	0.775	1.0	0.775	1.420	8.21	8.23	8.30(c)	8.30(d)
400 + 1A	0.568	1.00	0.568	1.116	9.12	9.11	9.13(c)	9.15(d)

* First number is peak transmission wavelength in mμ; second number is auxiliary filter designation.

** Based on observed lead aside initiation delays.

*** See Eqs. (2) and (3). $T_A = 28,000°K$, $T_{N_2} = 11,000°K$; $\epsilon_A = \epsilon_{N_2} = 1.00$.

(a) C_{rel} is very insensitive to T_A if T_A ~25,000° to 30,000°K.

(b) Some unknown absorbance in this fairly complex optical path reduces the P.M. output for $\lambda \leq 400$ mμ. This reduction is not found in the directly viewed "small-scale" shots. (Table 3)

(c) $T_A = 28,500°K$; $T_{N_2} = 11,100°K$

(d) $T_A = 29,000°K$; $T_{N_2} = 11,200°K$.

For the observed steady shock velocity of 8.1 mm/μsec, theoretical T_{N_2} is between 11,000 and 11,200°K (References 4 and 5).

Table 5

PVA LEAD AZIDE* INITIATION DELAYS

(4" x 4" x 8" 749 Mirror Boxes)

Shot No.	Packing Density (g/cc)	Confinement	Filter	Relative Intensity**	Initiation Delay (μsec)	Remarks
9,884	2.34	Glass(a, b)	None	-	1.02(b)	
	~2.4	Glass(a)	None	-	0.89	
	2.42			-	0.86	
	2.43			-	0.87	
	~2.4			-	0.91	
	2.42	Quartz		-	0.66	
	2.48	Quartz		-	0.70	
	2.48	Glass(a)	0-52	-	1.46	
	2.46	Glass(a)	0-52	-	1.48	
9,885	2.40	Glass(a)	None	-	0.98	
	~2.4			-	0.92	
	2.32			-	0.94	
	2.34			-	1.05(b)	
	~2.4			-	0.95	
	~2.4			-	1.07(b)	
	2.50		0-52	-	1.68	
9,896	~2.4-2.5	Glass(a)	None	-	0.86	
				-	0.88	
				-	0.84	
	2.51	None	Glass(a)	-	1.46	15-mil separation
	2.52			-	1.68	15-mil separation
	2.48			-	1.70	15-mil separation; 10-μ vacuum
	2.47			-	1.79	15-mil separation; 10-μ vacuum
9,936	2.53	Glass(a)	None	0.94	0.80	
	2.38				0.80	
	2.48				0.79	
	2.35				0.87	
	~2.4				0.79	
					0.82	
					0.78	
					0.78	
					0.80	
9,937	~2.4-2.5	Glass(a)	None	0.82	5.30	Truncated pyramid
					5.62	Mirror box
					3.48	
					5.88	
					5.98	
					6.02	
	2.45	Quartz			2.50	
	2.50	Quartz			2.72	
	~2.4	Glass(a)	0.1 ND		7.32	
	~2.4	Glass(a)	0.1 ND		7.44	
10,008	~2.4-2.5	Glass(a)	None	0.97	0.91	
					0.96	
					0.94	
10,009	2.4-2.5	Glass(a)	None	0.89	0.98	
	2.4-2.5				0.97	
	2.46				0.97	
	2.44				1.06(b)	
	2.4-2.5				0.98	
	2.30	None	Glass(a)		2.49	In press, holder; 1 atm, ~100-mil separation
	2.40				2.83	In press, holder; 1 atm,
	2.44				2.15	In press, holder; 21 atm N_2
	2.52				2.39	In press, holder; 21 atm N_2
10,043	~2.4	Glass(a)	None	0.97	0.81	4" u.v. reflecting box
					0.77	
					0.77	
		Quartz			0.42	
10,053	~2.4	Glass(a)	None	1.00	0.72	4" u.v. reflecting box
		Glass(a)			0.76	4" u.v. reflecting box
		Crown Glass			0.84	

* Granular PVA lead azide in standard assembly (See Experimental Section)

** From photomultiplier records, see Table 4

(a) 37-39-mil-thick microscope slides

(b) Glass poorly attached to azide holder

Table 5 (Continued)

Shot No.	Packing Density (g/cc)	Confinement	Filter	Relative Intensity[a]	Initiation Delay (μsec)	Remarks
10,167	~2.4	Glass(a)	None	- - - - - -	0.98 1.05(b) 1.02(b) 1.06(b) 1.11(b) 1.06(b)	
10,168	~2.3	Glass(a)	None	0.86	0.88 0.82 0.91	4" u.v. reflecting box
10,178	~2.3	Glass(a)	None	0.83	1.08 1.08 1.08	
10,179	~2.3	Glass(a)	None	1.00	9.24 9.18 9.00 10.15(c)	N_2 flash
10,195	~2.4	Glass(a)	None	- - -	0.95 1.02 1.00(a)	Plane surface shot
10,201	~2.4 ~2.4	Glass(a)	None	-	0.93 0.94	
10,202	~2.4	Glass(a)	None	- - -	0.98 0.96 1.07(a)	
10,218	~2.3 ~2.3	Glass(a)	None	-	1.08 1.08	
10,238	~2.4 ~2.4	Glass(a)	None	0.95 0.95	0.88 0.98	
10,245	~2.4 ~2.4	Glass(a)	None	- -	1.05 1.09	Plane surface shot
10,264	2.35 2.34 2.32	Glass(d)	None	1.00	0.82 0.84 0.86	
10,278	2.32 ~2.3 ~2.3	Glass(d)	None	- - -	0.80 0.86 0.92	Plane surface shot
10,429	~2.3 2.36 ~2.3	Glass(d)	None	0.79	1.04 1.11 1.07	
10,434	~2.3	Glass(d)	None	- - -	0.92 1.02 1.00	Plane surface shot
10,452	~2.3	Glass(d)	None	- - -	0.95 0.94 0.98	Plane surface shot
10,454	~2.3 ~2.3	Glass(d)	None	- -	0.90 0.89	Plane surface shot
10,473	~2.3 2.40 ~2.3 ~2.3 ~2.3 2.30 ~2.3 ~2.3 2.34 ~2.3	Glass(d)	None	0.83	1.00 1.06 1.02 0.94 1.03 1.09 1.02 1.05 1.11 1.16 1.04 1.10 1.24	15° from vertical 30° from vertical 40° from vertical

(a) 37-39-mil-thick microscope slides
(b) Glass poorly attached to aside holder
(c) Shaded by Tedlar foil used in measuring shock velocity
(d) 29-mil-thick microscope slides

Table 5 (Continued)

Shot No.	Packing Density (g/cc)	Confinement	Filter	Relative Intensity[a]	Initiation Delay (μsec)	Remarks
10,510	~2.3	Glass(d)	None	0.95	0.73 0.82 0.82 0.93	4" w.v. reflecting box 30° from vertical
10,511	~2.3 ~2.3	Glass(d)	None	0.81 0.81	1.06 1.06	Curved surface shot
10,515	2.30 2.31	Glass(d)	None	- -	0.93 0.89	Curved surface shot
10,530	~2.3 ~2.3	Glass(d)	None	- -	1.05 1.11	Plane surface shot
10,593	~2.4 2.39	Glass(d)	None	- -	0.96 0.95	Plane surface shot
10,594	~2.4	Glass(d)	None	- - -	0.87 0.84 0.87	Plane surface shot
10,595	~2.4 ~2.4	Glass(d)	None	- -	0.97 0.98	Plane surface shot
10,653	2.40 ~2.4 ~2.4	Glass(d)	None	- - -	0.82 0.90 0.80	Plane surface shot
10,654	~2.4 2.41 2.38 ~2.4	Glass(d)	None	0.99	0.85 0.86 0.83 0.88	
10,655	~2.4 ~2.4 ~2.4 2.39 2.39 2.38	Glass(d) None	None Glass(c)	1.00	9.80 9.17 8.95 8.93 8.88 9.02	N_2 flash 1-mil separation
10,682	~2.4 2.39 ~2.4 2.39 2.40	Glass(d) None	None Glass(c)	1.00	1.02 0.96 1.00 1.39 1.54	No sun tan 1-mil separation
10,683	2.36 ~2.4 ~2.4	Glass(d)	None	1.00	0.98 0.99 0.98	No sun tan
10,807	~2.4 ~2.4	Glass(d)	None	- -	0.93 0.98	Plane surface shot
10,808	~2.4	Glass(d)	None	0.96	0.86 0.90 0.88	
10,828	~2.4 2.36	Glass(d)	None	- -	0.88 0.94	Plane surface shot
10,829	~2.4 2.36	Glass(d)	None	- -	0.86 0.82	Curved surface shot
10,862	~2.4 ~2.4	Glass(d)	None	- -	1.09 0.98	Curved surface shot
10,863	~2.4	Glass(d) None	None None 0.3 ND Glass(d) Glass(d) PVF-40	- - - - - - -	0.86 0.90 1.65? 3.74 4.05 1.71 1.54 1.16	 1-mil separation "Old" aside; 1-mil separation 1-mil separation
10,874	~2.4	Glass(d)	None	-	0.91	Curved surface shot
10,875	~2.4	Glass(d)	None	-	0.76?	Curved surface shot

(d) 29-mil-thick microscope slides
(e) 34-mil-thick microscope slides

Table 5 (Continued)

Shot No.	Packing Density (g/cc)	Confinement	Filter	Relative Intensity[aa]	Initiation Delay (μsec)	Remarks
10,947	2.04	Glass(d, f)	None	-	0.96	Curved surface shot
	3.33			-	1.04	
	~3.4			-	1.37	
10,948	2.36	Glass(d, f)	None	-	0.95(b)	Curved surface shot
	2.06			-	0.88	
	3.66			-	1.37	
	3.73			-	>1.05	Some oxide fell out
11,011	2.20	Glass(d)	None	-	0.88	
	2.28	Glass(d)		-	0.86	
	3.80	Glass(d, f)		-	1.23	
	3.70	Glass(d, f)		-	1.27	
	3.74	None	Glass(d)	-	1.57	1-mil separation
	3.60	None	Glass(d)	-	2.03	1-mil separation
11,177	2.43	Glass(d)	None	0.95	0.84(g)	
	2.36	Glass(d)			0.83(g)	
	~2.4	Glass(d, b)			0.94(g, b)	
	3.82	4-mil PVF	Glass(d)		1.30(g)	
	~4.1	4-mil PVF			1.57(g)	
	3.66	None			1.28(g)	8-mil separation
	3.68				1.71(g)	no sleeve
	~3.7				1.75(g)	
	2.41	1-mil PVF	None		0.75(g)	
11,178	~2.4	Glass(d)	None	0.80	0.88(g)	
	2.47				0.86(g)	
	2.39				0.81(g)	
	2.44	Quartz			0.81(g)	
	2.35	1-mil PVF			0.76(g)	
	2.33	1-mil PVF			0.73(g)	
	4.13	None	Glass(d)		2.25(g)	9-mil separation
	2.40		1-mil PVF		1.28(g)	23-mil separation
	2.40		1-mil PVF		1.23(g)	23-mil separation
11,223	~2.4	Glass(d)	None	-	0.82(g)	Curved surface shot
	~2.4			-	0.86(g)	
11,224	~2.4	Glass(d)	None	1.00	0.86(g)	
	2.42				0.80(g)	
	~2.4				0.84(g)	
	3.10	4-mil PVF	Glass(d)		1.23(g)	
	3.09				1.11(g)	
	4.40				2.01(g)	
	4.28				1.97(g)	
	4.25	None			2.21(g)	12-mil separation
	4.16	None			2.19(g)	13-mil separation
11,225	2.39	Glass(d)	None	1.00	10.50(g)	N_2 flash; cracked glass
	~2.4				9.52(g)	
	2.41				8.71(g)	
	2.43				9.05(g)	
	2.42	Quartz			6.38(g)	
	2.38	Quartz			6.44(g)	
	3.20	4-mil PVF	Glass(d)		13.28(g)?	poor sum tan
	2.41	None			9.95(g)	1-mil separation
	2.35				9.31(g)	1-mil separation
	2.45				11.99(g)	30-mil separation
	2.46				11.26(g)	30-mil separation
	~3.7				11.69(g)	8-mil separation
	~3.4				9.09(g)?	4-mil(?) separation

(b) Glass poorly attached to oxide holder
(d) 29-mil-thick microscope slides
(f) Confinement attached to loaded assembly
(g) Mirror box reflectivity in these shots was greater than previously. All delays have been normalized to a standard delay of 0.84 μsec.

Table 5 (Concluded)

FVM No.	Peaking Density (g/cc)	Confinement	Filler	Relative Intensity**	Initiation Delay (μsec)	Remarks
11,236	~2.4	Glass(d)	None	0.91	2.13(b)	4" Black box; rubber under glass
	~2.4				1.82	
	~2.4				1.78	20½° from vertical
	~2.4				1.92	34° from vertical
	2.34	Quartz			0.68	
	2.34	Quartz			0.65	
	3.20	4-mil PVF	Glass(d)		?.??	
	4.23	4-mil PVF			4.00	
	2.30	None			2.92	1-mil separation
	2.34				2.89	1-mil separation
	2.38				3.30	14-mil separation
	2.34				3.88	
	4.12				4.85	
11,241	~2.4	Glass(d)	None	0.95	0.83(g)	Curved surface shot
	~2.4				0.85(g)	
11,242	2.42	Glass(d)	None	0.93	0.88(g)	Curved surface shot
	~2.4			0.93	0.84(g)	
11,243	~2.4	Glass(d)	None	0.92	0.82(g)	Curved surface shot
	~2.4			0.92	0.86(g)	
11,244	~2.4	Glass(d)	None	1.00	0.80(g)	Curved surface shot
	~2.4			1.00	0.83(g)	
9,884	2.46	1/3-mil Mylar	None	-	1.15	
	2.48	1/3-mil Mylar(b)?	None	-	1.41	
9,885	2.42	1/3-mil Mylar	None	-	1.33	
	2.33	4-mil Tedlar	None	-	1.47	
		4-mil Tedlar	None	-	1.88	
9,894	2.51	None	None	-	1.20	
	2.41	↓	↓	-	1.19	
9,895	2.38	None	None	-	1.16	
	2.43	↓	↓	-	1.15	
9,896	2.39	None	None	-	0.97	
	2.47	↓	↓	-	1.03	
	-			-	1.01	
	~2.3			-	1.01	"Old" aside
	~2.3			-	1.03	↓
	~2.3	↓	↓	-	0.93	
9,936	2.37	None	None	0.96	0.79	4" Box; new loadings
	2.37	↓	↓	↓	0.80	↓
	2.40				0.82	
	2.36	↓	↓	↓	0.82	↓
9,937	2.38	None	None	0.82	4.34	Truncated pyramid box
10,008	2.47	None	None	0.97	1.03	4-minute sun tan
	2.47				0.97	↓
	2.29				1.02	
	2.34				0.99	
	2.35				0.97	↓
	2.37				1.01	1 1/2-minute sun tan
	2.40				0.96	1 1/2-minute sun tan
	~2.4				1.00	No sun tan
	~2.3				11.1 !	4-minute sun tan; very old aside
	~2.3	↓	↓	↓	3.33	4-minute sun tan; very old aside
10,009	2.50	None	None	0.89	1.02	
	2.40	↓	↓	0.89	1.12	

(b) Glass poorly attached to aside holder
(d) 29-mil-thick microscope slides
(f) Confinement attached to loaded assembly
(g) Mirror box reflectivity in these shots was greater than previously. All delays have been normalized to a standard delay of 0.84 μsec.

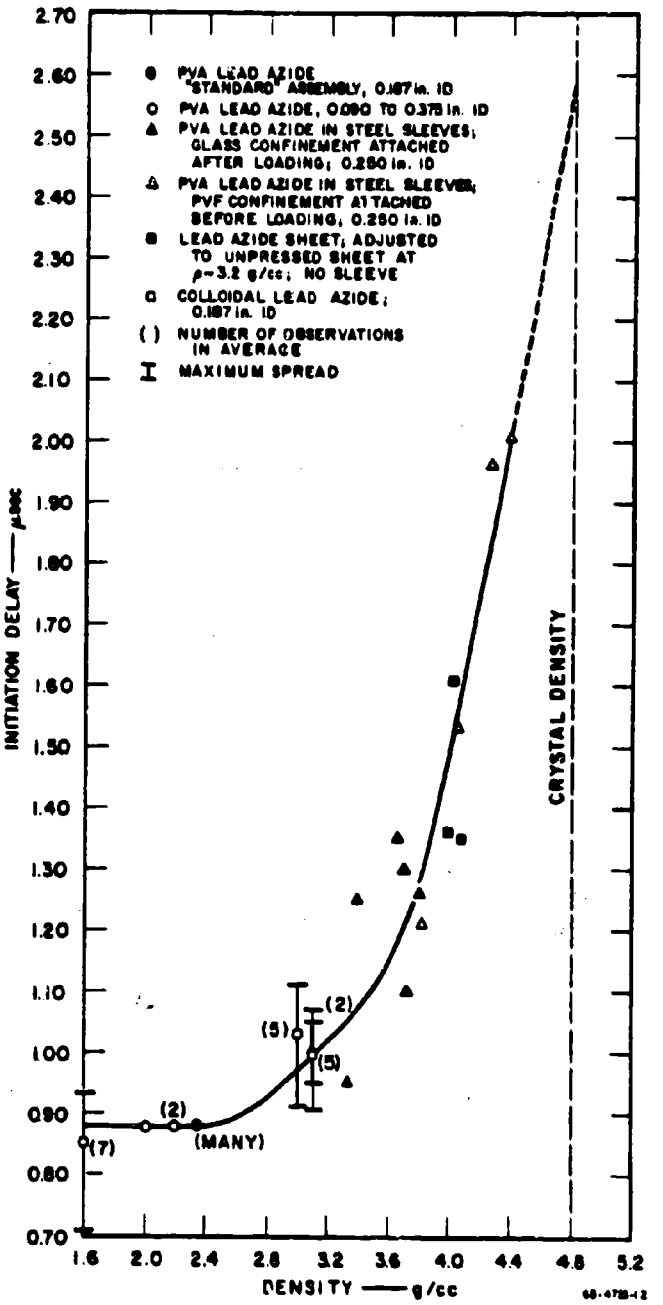

Figure 10 INCREASE IN INITIATION DELAY OF LEAD AZIDE WITH INCREASING PACKING DENSITY

developed, are listed in Table 6. As already mentioned (see Sec. II-2c) some difficulties are still encountered in attaching confinement. The fairly large jitter shown in Table 6 is undoubtedly a consequence of this. The results in Table 6, and more clearly in the summary Table 7, indicate all batches except 7, 8, and 13 have about the same normalized initiation delay. Delays for Batch 7 are shorter than the others, and those for Batches 8 and 13 are longer. Batch 7 was made with colloidal lead azide. The duPont Company informed us that they experienced considerable difficulty in mixing colloidal azide and binder prior to the fabrication of the sheet. It is believed that Batch 7 has a lower binder content and Batches 8 and 13 a higher binder content than usual. This view is supported by the observation that for a given sun exposure Batch 7 turned more brown (sun tanned) and Batch 8 less brown than the other batches.

e. Initiation of plane surfaces

The assembly of plane surface initiation shots was described in Sec. II-2b and depicted in figures 5 and 6. In all these shots (as well as the curved surfaces to be discussed in the next section) the explosive face toward the smear camera was viewed by a multi-slit arrangement as shown in the "still" of figure 11. Generally 9 to 12 slits traversed the explosive surface. In an ideal surface initiation the smear record should look just like the still, i.e., all the slits should be lit up simultaneously along their entire length. Figure 11 shows a record in which this ideal situation is approached. Figure 12 shows a shot in which the simultaneity of detonation is not as good as that in figure 11, presumably because the window was not in as good contact with the azide sheet.

Table 8 presents the analysis of the shot shown in figure 11. Although this was one of the best shots from the point of view of small jitter, certain features in Table 8 are common to most plane-wave shots. Note the increased initiation delay at the outer periphery of the explosive ("Top," "Bottom," and slit 1). The jitter along any single slit is often smaller for the central slits than for the outer slits, as is the case for

Table 6

NORMALIZED INITIATION DELAYS OF LEAD AZIDE SHEET DISKS

Shot No.	Sheet Batch No.	Sheet Density (g/cc)	Confinement	Normalization Factor	No. of Obs.	Average Normalized Delay (μsec)	Range (μsec)
10,948	10	3.0	37-mil Glass	0.97	2	1.44	1.42-1.46
10,947	10	2.9		0.87	1	1.40	-
10,911	10	~3.2		?	2	1.56(a)	1.53-1.56(a)
10,875	10	~3.3		1.00	2	1.30	1.28-1.31
10,874	10	~3.3		0.925	4	1.47	1.45-1.49
10,862	9	3.2		0.86	1	1.54	-
10,808	9	~3.2		0.955	2	1.44	1.42-1.46
10,807	9	~3.2		0.86	1	1.44	-
10,434	6	~3.2		0.875	1	1.46	-
10,245	3	~3.0		0.825	2	1.43	1.42-1.44
11,244	13	3.1	29-mil Glass	1.00	2	2.12	2.07-2.17
11,224	13	3.05		1.00	2	2.20	2.20-2.20
11,241	12	3.12		0.94	3	1.47	1.42-1.50
11,223	12	3.18		0.99	1	1.49	-
11,118	12	3.21		0.89	1	1.41	-
11,177	12	3.16		0.93	1	1.48	-
11,178	11	3.09		0.89	1	1.45	-
11,177	11	3.00		0.93	2	1.43	1.38-1.47
11,011	5	3.00		0.98	4	1.37	1.33-1.42
11,011	6	3.12		0.98	1	1.39	-
11,011	8	3.06		0.98	2	1.53	1.51-1.55
10,863	10	3.2		0.955	1	1.33	-
10,808	9	~3.2		0.955	1	1.45	-
10,429	5	~3.2		0.80	3	1.32	1.31-1.34
10,429	6	~3.2		0.80	2	1.39	1.36-1.41
10,828	9	~3.2	4-mil Glass	0.925	2	1.23	1.17-1.30
10,875	10	~3.3	4-mil PVF-40	1.00	2	1.43	1.42-1.43
10,862	9	3.2		0.86	1	1.57	-
10,829	9	~3.2		1.00	2	1.42	1.39-1.45
10,594	8	~3.2		0.975	2	1.75	1.69-1.85
10,683	9 & 10	~3.2	4-mil Tedlar	1.00	3	1.32(b)	1.30-1.36(b)
10,683	3	~3.2		1.00	2	1.28(b)	1.27-1.28(b)
10,683	5	~3.2		1.00	2	1.38(b)	1.34-1.42(b)
10,683	8	~3.2		1.00	2	1.54(b)	1.46-1.63(b)
10,682	9	~3.2		0.965	2	1.32(b)	1.30-1.34(b)
10,682	10	~3.2		0.965	1	1.31(b)	-
10,654	6	~3.2	4-mil Tedlar	0.995	1	1.25	-
10,654	7	~3.2		0.995	1	1.02	-
10,593	7	~3.2		0.88	1	0.99	-
10,538	7	~3.2		0.72	2	1.04	1.01-1.08
10,513	5	~3.2		0.93	3	1.37	1.32-1.40
10,454	6	~3.2		0.93	1	1.38	-
10,452	5	~3.2		0.875	1	1.35	-
10,434	6	~3.2		0.80	1	1.33	-
10,429	5	2.5	None	0.80	2	2.94	2.54-3.34
10,429	6	2.5	None	0.80	2	4.55	4.10-4.90
10,178	1	<3	None	0.815	2	4.22	3.94-4.50
10,178	2	<3	None	0.815	2	3.97	2.85-3.10

(a) Not normalized.
(b) Not sun-tanned; corrected to 4 min. sun tan to which all other disks were exposed.

Table 7

SUMMARY OF NORMALIZED INITIATION DELAYS
FOR LEAD AZIDE SHEET DISKS

Batches	No. of Shots	No. of Obs.	Confinement	$\bar{\tau}$ (μsec)	Range (μsec)	B_o* (°K/μsec)	B (°K/μsec)	$\Delta\bar{\tau}$** (μsec)	$B(\bar{\tau} - \Delta\bar{\tau})$ (approx.) (°K)
5, 6, 9, 10	3	12	29-mil G	1.36	1.31-1.45	1370	820	0.18	970
11, 12	3	8	29-mil G	1.46	1.41-1.50	1370	820	0.17	1050
3, 6, 9, 10	8(a)	14	37-mil G	1.45	1.42-1.54	1300	800	0.18	1020
9	1	2	4-mil G	1.23	1.17-1.30	1580	~800	0.15	~ 900
8	1	2	29-mil G	1.53	1.51-1.55	<1370	<830	0.13	<1160
13	2	4	29-mil G	2.16	2.07-2.20	-	-	-	-
9, 10	2(b)	4	PVF-40; 4-mil	1.42	1.39-1.45	1825	810	0.20	985
8	1	2	PVF-40; 4-mil	1.75	1.69-1.85	<1825	<835	0.20	<1280
7	3	4	Tedlar; 4-mil	1.03	0.99-1.08	~2445	915	0.20	770
3, 5, 6, 9, 10	7	17	Tedlar; 4-mil	1.34	1.25-1.42	~2445	~990	0.20	~1130
8	1	2	Tedlar; 4-mil	1.54	1.46-1.63	~2445	~1020	0.20	<1350
1, 2, 5, 6	2	8	None	3.66	2.54-4.90	≈6000	-	<0.1	-

* Integral of Eq. 5 divided by c_v
** From figure 10
(a) Omitting Shots 10,911 and 10,875.
(b) Omitting value from Shot 10,862.

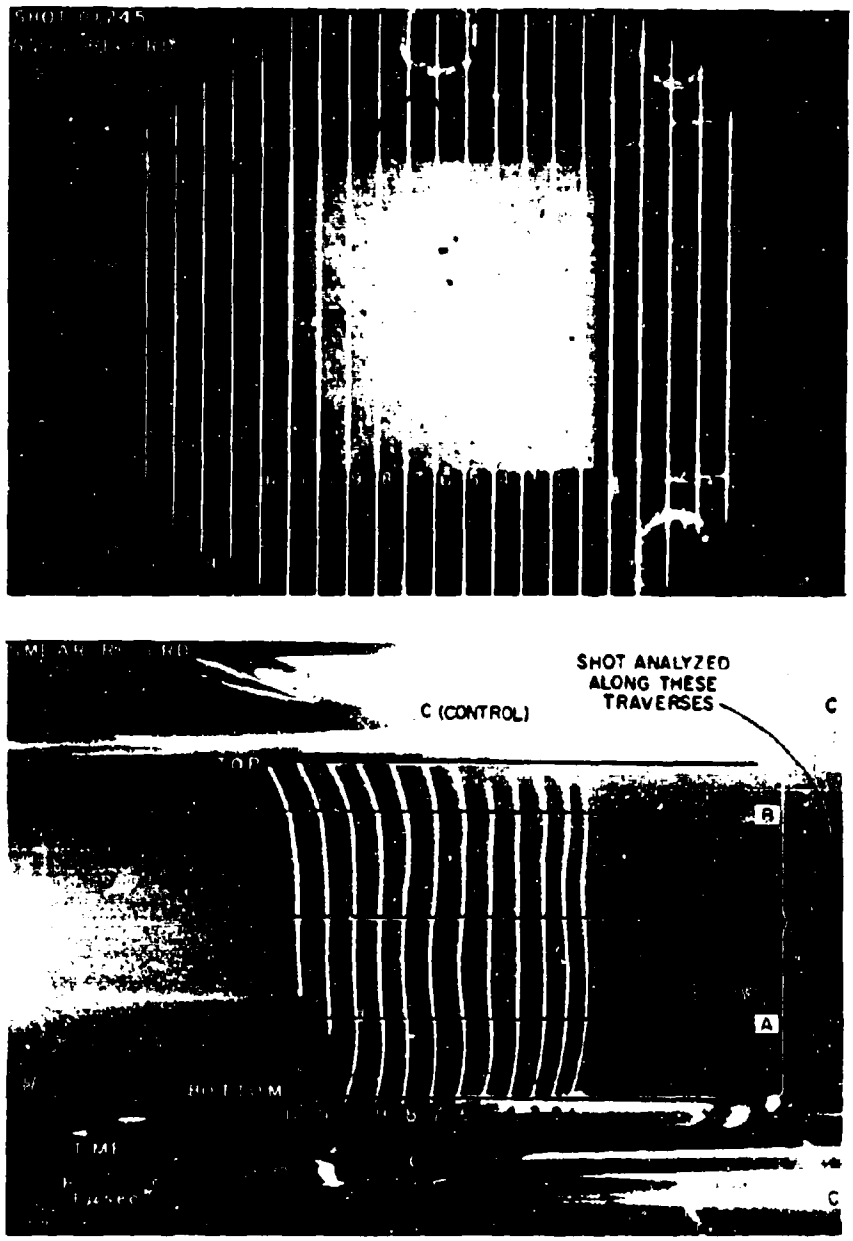

Figure 11 PLANE-WAVE SHOT, SHOT 10,245

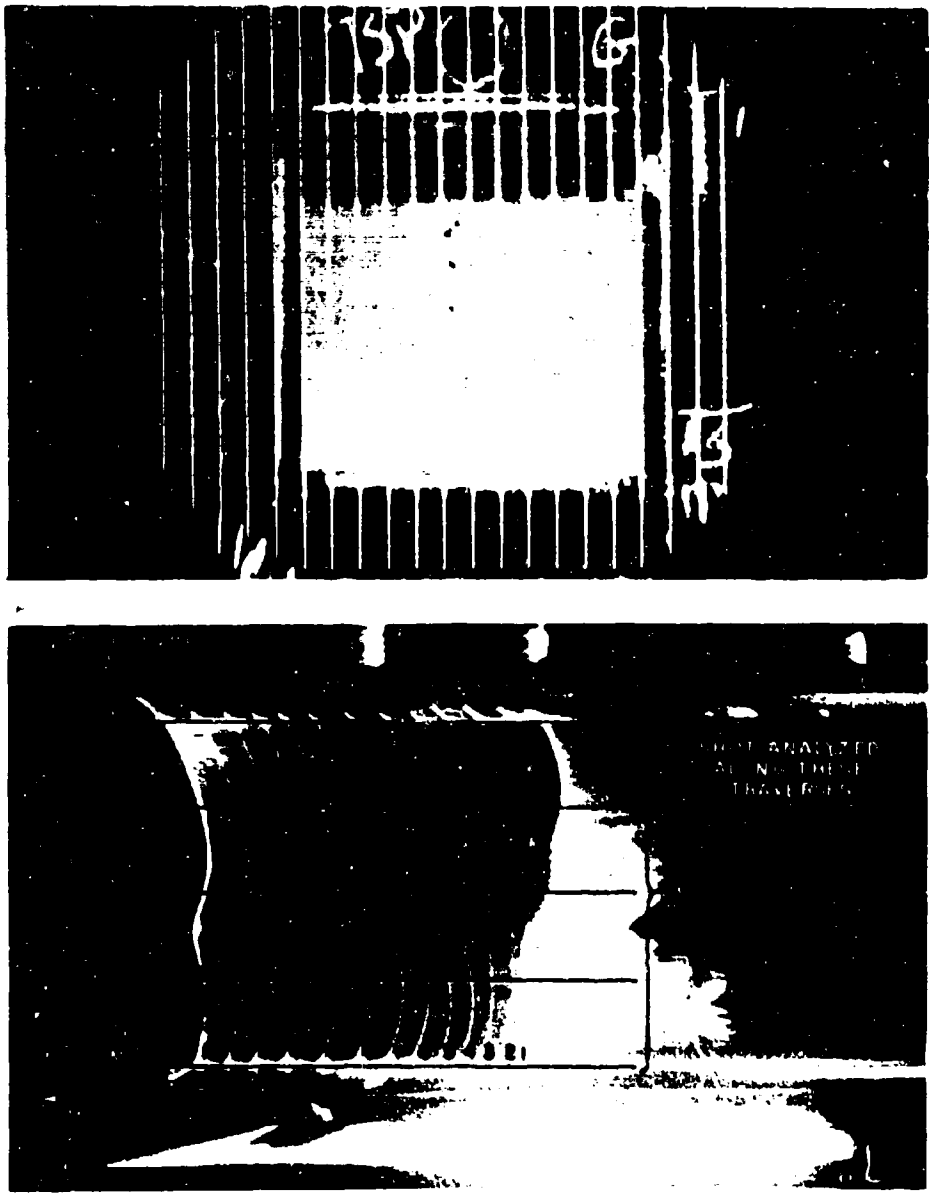

Figure 12 PLANE-WAVE SHOT, SHOT 10,454

Table 8

ANALYSIS OF PLANE WAVE SHOT NO. 10,245

Slit Position	Total Delay from Start of Argon Flash (μsec)														
	1	2	3	4	5	6	7	8	9	10	11	12	Avg	Jitter	Standard Deviation
Bottom	4.78	4.68	4.60	4.57	4.54	4.52	4.49	4.47	4.48	4.49	4.49	4.54	4.55	0.31 0.21(a)	0.09 0.06 (a)
A*	4.65	4.55	4.47	4.45	4.42	4.42	4.42	4.40	4.36	4.35	4.34	4.35	4.43	0.30 0.20(a)	0.09 0.06 (a)
Center	4.60	4.50	4.43	4.41	4.41	4.42	4.44	4.41	4.37	4.35	4.34	4.35	4.42	0.26 0.16(a)	0.07 0.045(a)
B*	4.55	4.45	4.40	4.38	4.38	4.35	4.35	4.35	4.35	4.34	4.35	4.38	4.39	0.21 0.11(a)	0.06 0.03 (a)
Top	4.61	4.55	4.50	4.49	4.46	4.49	4.48	4.51	4.55	4.54	4.56	4.60	4.53	0.15 0.14(a)	0.05 0.04 (a)
Jitter	0.22	0.23	0.20	0.19	0.16	0.14	0.14	0.16	0.18	0.20	0.22	0.25	-		

Overall average delay = 4.46 μsec
Overall standard deviation = 0.096 μsec
Overall jitter = 0.44 μsec

Modified(b) overall average delay = 4.40 μsec
Modified(b) overall standard deviation = 0.05 μsec
Modified(b) overall jitter = 0.21 μsec

* See Fig. 11
(a) Omitting Slit 1
(b) Omitting Slit 1 and bottom and top

the shot shown. The jitter along a single slit, along any row, or overall, is four to five times greater than the corresponding standard deviation from the mean, which according to the usual statistical considerations indicates a randomly distributed variability of initiation delay. For example, the shot of figure 12, which is one of the worst, has an overall jitter of 0.57 μsec and an overall standard deviation from the mean of 0.14 μsec; without "edges" the jitter and standard deviation are 0.50 and 0.12 μsec, respectively.

The overall average initiation delays, $\bar{\tau}$, the average of the shortest initiation delays for every slit, $\bar{\tau}_{min}$, the overall jitter, and the overall jitter without "edges" are shown for all plane-wave shots in Table 9. With the exception of the unconfined or poorly confined shots, $\bar{\tau}$ and $\bar{\tau}_{min}$ are not very different. As was found for control disks, surface-initiation shot delays using Batch 7 sheet azide are shorter and those using Batch 8 or 13 are longer than shots using the other batches. The average initiation delays are not very strongly influenced by the type of confinement used. This observation will be discussed later. The greater jitter at the "edges" has already been mentioned. The results shown make it obvious that good (i.e., reproducibly applied) confinement greatly reduces jitter. Further study of these data shows that in systems of comparable confinement jitter is smaller for the thicker explosive trains. The same effect is observed if one compares the light-breakout pattern for a thin explosive train with that observed when the shock generated by the same explosive train travels through about 1/8 inch of Lucite and becomes luminous, when it then enters a very thin argon gap. This is shown in figure 13. The earlier light breakouts, which are numbered, correspond to the directly viewed detonation, and the later set, which partially overlaps the first signals, corresponds to the attenuated shock. Here the overall jitters before and after passage through the Lucite are 0.50 and 0.42 μsec, and the corresponding "without edges" jitters are 0.48 and 0.30 μsec. In other records this effect is even more pronounced. These observations are consistent with the supposition that the leading portions of a ragged shock profile are attenuated more

Table 9

SURFACE INITIATION SUMMARY

Shot No.	Sheet Azide Batch	Confinement	$\bar{\tau}$ (μsec)	$\bar{\tau}_{min}$ (μsec)	Overall Jitter (μsec)	$1\frac{1}{2} \times 1\frac{1}{2}$" Jitter (μsec)	B_o (°K/μsec)	B (°K/μsec)	Density Correction $\Delta\bar{\tau}$ (μsec)	$B(\bar{\tau}_{min} - \Delta\bar{\tau})$ (°K)
Plane Surfaces										
9,471	1 or 2(a)	29-mil glass(d)	1.73	1.52	0.60	0.46	1370	860	-	-
10,167	1 or 2(a)	None	~13	12.9	2.01	-	-	-	-	-
10,245	3(a)	29-mil glass	1.37	1.32	0.44	0.18	1370	810	0.20	905
10,828	9(b)	34-mil glass	1.32	1.19	0.50	0.48	1730	942	0.20	995
10,278	4(a)	4-mil Tedlar	1.35	1.27	0.46	0.28	~2450	~ 975	0.20	~1040
10,436	6(a)	4-mil Tedlar	1.29	1.23	0.52	0.34	~2450	~ 975	0.40	~1000
10,452	5(a)	4-mil Tedlar	1.25	1.20	0.50	0.31	~2450	~ 975	0.20	~ 900
10,456	6(a)	4-mil Tedlar	1.58	1.45	0.57	0.50	~2450	~1000	0.20	~1250
10,538	7(b)	4-mil Tedlar	1.06	0.93	0.70	0.70	~2450	~ 900	0.20	~ 660
10,593	7(c)	4-mil PVF	1.16	1.09	0.30	0.25	1825	755	0.20	670
10,594	8(b)	4-mil PVF (d)	2.26	1.92	1.30	1.30	1825	860	0.20	1480
10,807	9(b)	4-mil PVF	1.49	1.33	0.91	0.65	1825	790	0.20	980
Hemicylindrical Surfaces										
10,874*	10(c)	82-mil glass	1.67(e)	1.44(e)	0.60	0.30(f)	1470	865	0.18	1090
10,867*	10(b)	82-mil glass	1.81(g)	1.67(g)	0.90	0.57(f, g)	1470	-	0.16	-
10,511*	5(b)	4-mil Tedlar(d)	-	~1.35(h)	~0.9	-	~2450	-	0.2K	-
10,512*	6(b)	4-mil Tedlar(d)	-	<1.35(h)	1.02	0.96	~2450	~ 950	0.18	<1130
10,513*	5(b)	4-mil Tedlar(d)	~2.1(h)	1.43(h, i)	0.75	0.37(f)	~2450	~1000	0.20	~1300
10,911*	10(b)	4-mil PVF	1.31	1.29	1.44(j)	1.42(f, j)	1825	790	0.20	850
10,968*	8(c)	4-mil PVF	-	1.51	0.87	0.52(f)	1825	~ 850	0.29	~1060
10,862**	9(b)	102-mil glass	1.60(e)	1.44(e)	0.61	0.28(f)	1390	815	0.18	1060
10,875**	10(b)	102-mil glass	1.65(e)	1.47(e)	0.86	0.43	1390	815	0.17	1060
11,266***	13(b)	82-mil glass	2.01	1.91	0.77(k)	0.33	1470	880	0.10	~1690
11,262***	11(b)	1-mil PVF(m)	1.63	1.47	1.10(l)	0.51	1840	970	0.17	1260
11,263***	12(b)	1-mil PVF	1.77	1.64	0.60(k)	0.60	1840	970	0.18	1220
11,261***	12(b)	4-mil PVF(m)	(l)	1.27	-	large	1825	790	0.15	885

* 27.5-mm radius of curvature
** 38-mm radius of curvature
*** 25-mm radius of curvature
(a) Sheet azide on 30-32-mil PETN sheet on 200-mil EL-506D on 500-mil Comp B
(b) Sheet azide on 30-34-mil PETN sheet
(c) Sheet azide on 30-32-mil PETN sheet on 60-mil EL-506D
(d) Poor confinement due to poor gluing techniques
(e) Glass is badly cracked
(f) Along any horizontal traverse
(g) Sheet azide not in complete contact with PETN sheet
(h) Poor records
(i) Not normalized
(j) Wrinkles in confinement
(k) A portion of confinement was loose
(l) Confinement is loose at edges, therefore overall jitter is very large and not meaningful
(m) Confinement attached to azide in curved mold

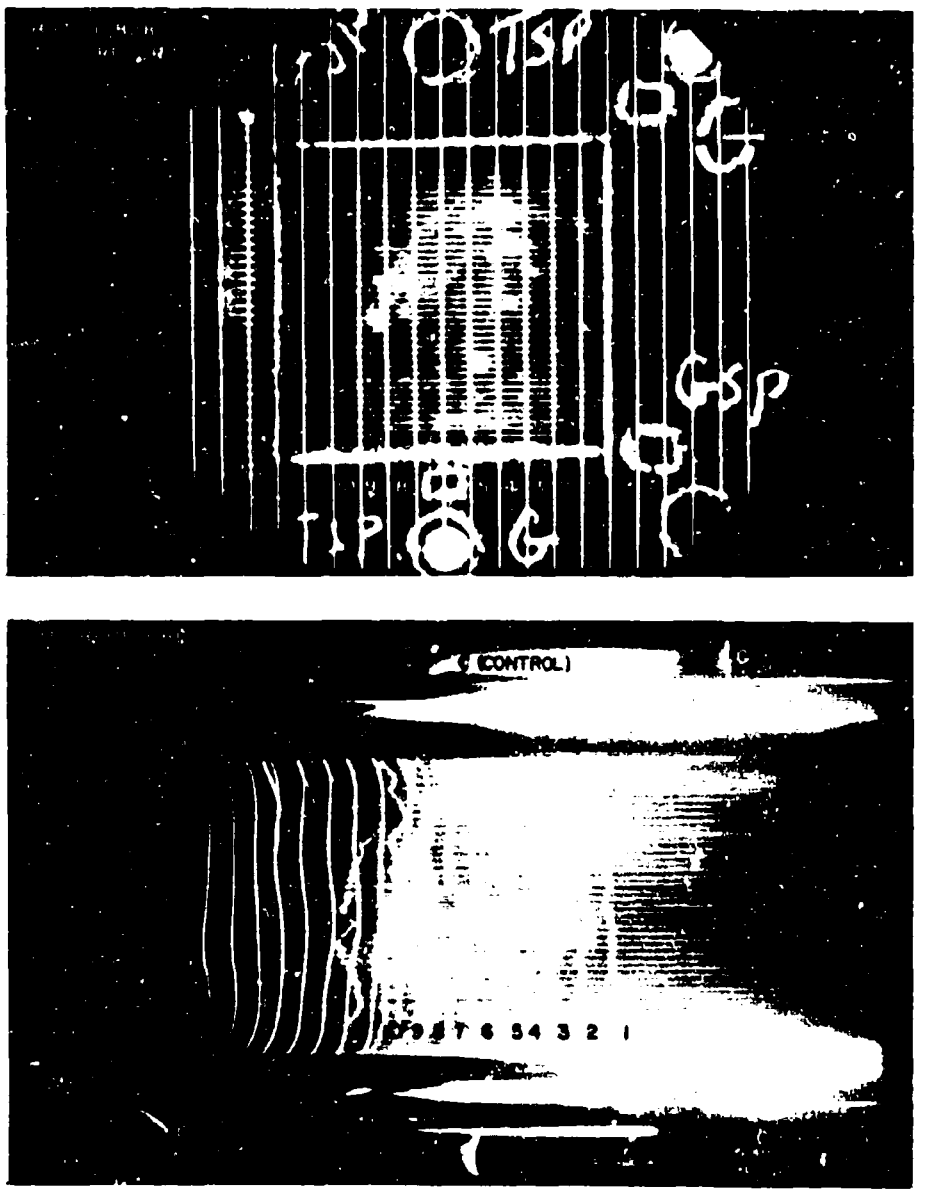

Figure 13 PLANE-WAVE SHOT, SHOT 10,828

by any medium, explosive or inert, through which the shock passes. From a practical point of view this is an important effect. It means that even a rather jittery shock can be appreciably smoothed before it enters a test structure which is being shock-loaded "simultaneously" along its surface if one interposes some relatively thin plastic sheath between the explosive and the test structure. It seems likely that any ablating material around the test structure will function in this manner.

f. Angle effect

Before summarizing the observations on surface initiation of cylinders, it is necessary to consider how initiation delay is influenced by tilting the lead azide surface to some angle α relative to the vertically positioned shot holder which is parallel to the advancing plane argon shock. If all the radiation arrived as a collimated beam, and if the azide surface acts as a Lambertian absorber, the fraction of radiation received by the azide would be proportional to its projected area and would be given by $\cos \alpha$. In reality some 70 to 80% of the energy is received via reflections and the radiation strikes the azide at all angles of up to about 60° so that a simple cosine law would not be expected to hold. Since the optics of the situation are very complex, an empirical approach was used to determine the magnitude of the angle effect. Standard assemblies were tilted at known angles from the vertical and initiated and recorded in the usual manner. Results are shown in figure 14. Although the experimental scatter is large, it is apparent that the angle effect is quite small for tilts of up to 30° or even 40°.

g. Surface initiation of hemicylinders

These results are summarized in Table 9. Here $\bar{\tau}$ and $\bar{\tau}_{min}$ differ from each other rather more than they did for flat surfaces. Often the overall jitter is greater than for flat surfaces, but is roughly comparable to flat surfaces if jitters are taken along any given horizontal traverse. A 27.5-mm radius of curvature hemicylinder (figure 15) appears to show a decidedly faster initiation in the central portions than for the outer portions.

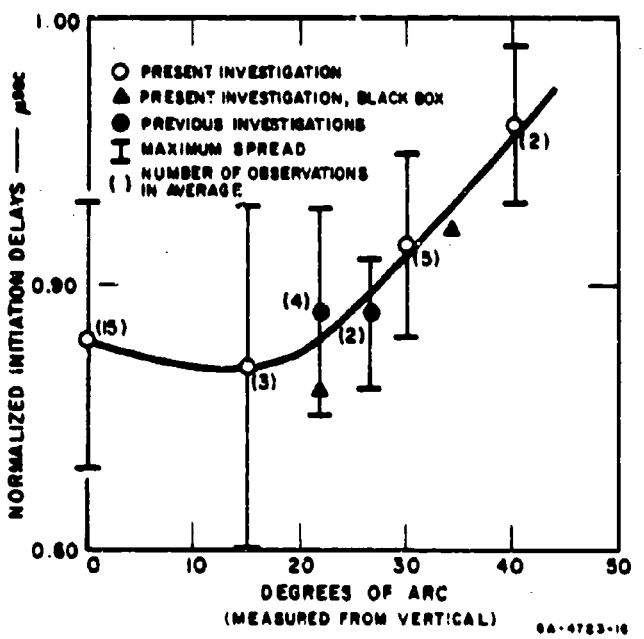

Figure 14 INFLUENCE OF TILT ANGLE ON INITIATION DELAY OF PVA LEAD AZIDE

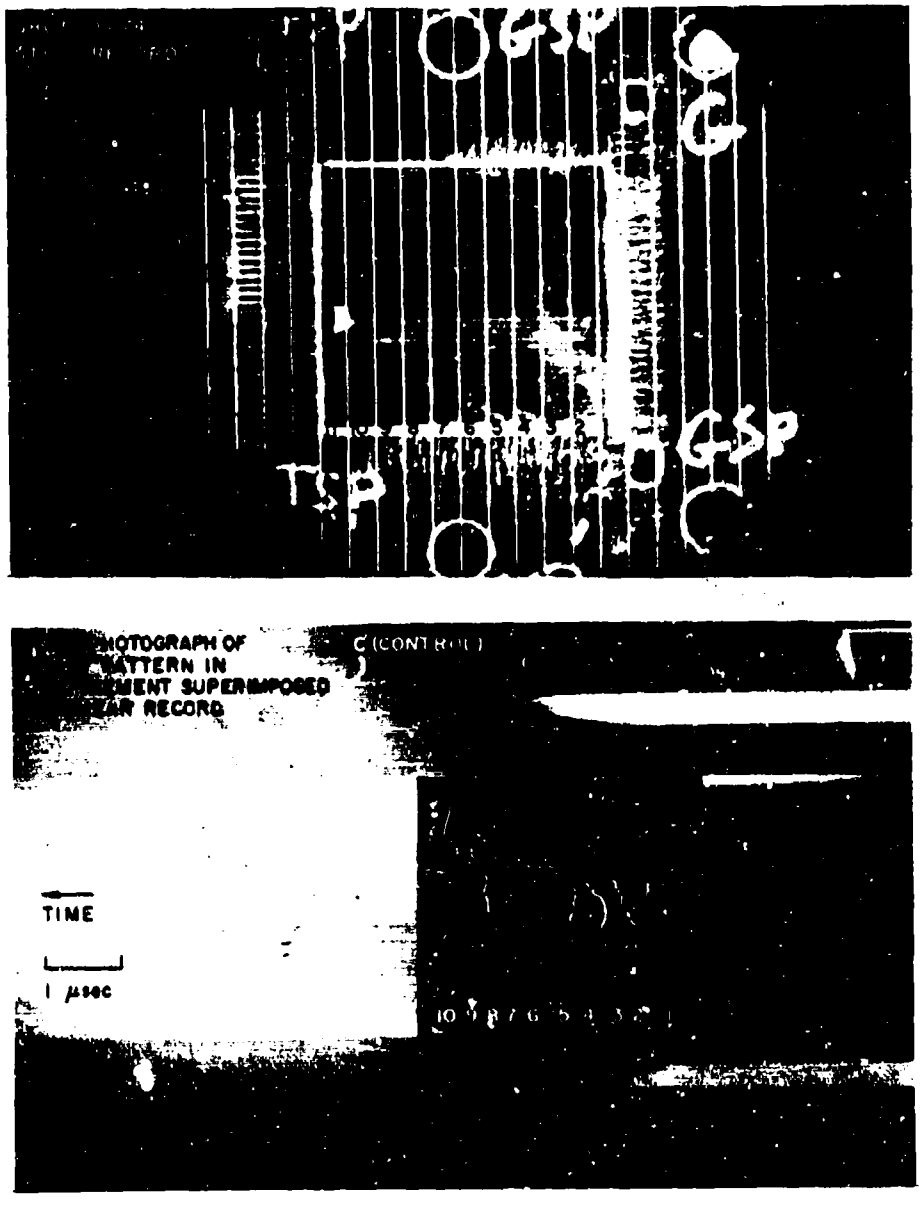

Figure 15 HEMICYLINDRICAL SHOT (27.5-mm Radius of Curvature)

For the more gradually curved surface of figure 16 this difference in initiation delay is less pronounced. The strongest argument against explaining these observations on the basis of the angle effect just discussed is furnished in figure 17. Here the radius of curvature was 25 mm so that the angle effect should have been quite pronounced, but initiation can be seen to occur uniformly over most of the viewed surface. There were no cracks in the glass confinement of this shot. For the shots in figures 15 and 16 the glass front-surface confinement was cracked during loading. Photographs of the crack pattern are superimposed on the smear records. Note the striking correspondence of crack location and increased initiation delay. Thus an appreciable fraction of the observed jitter in these shots is due to cracks in the confinement, and the apparent early initiation in the center of figure 15 is presumably due to crack location rather than any angle effect. Very close to the upper and lower portions of these records the tangents to the curved surfaces form angles of 30 to 40° from the vertical. The increased initiation delay observed in all three records for these regions may well be a manifestation of the angle effect.

The record of figure 17 also provides clear-cut evidence about the major cause of delay jitter. During shot assembly it was noticed that there was poor contact between azide and glass confinement in what is the lower right-hand region of the record, and to a lesser degree in the extreme left of the shot. These regions correspond exactly to the long delays seen on the lower portions of slits 1 and 2 and the jitter shown by the upper part of slit 9.

The results in Table 9 show a larger jitter for the shots confined with thin plastics than with glass. It is believed that this difference is primarily due to the difficulty of obtaining a good bond between the plastic and the sheet azide. In the regions of no bonding or weak bonding the azide and the plastic separate, the delay is increased, and this shows up as jitter. As will be shown later (Table 12), 1-mil-thick plastic is as good a confining agent as 40-mil glass for granular lead azide.

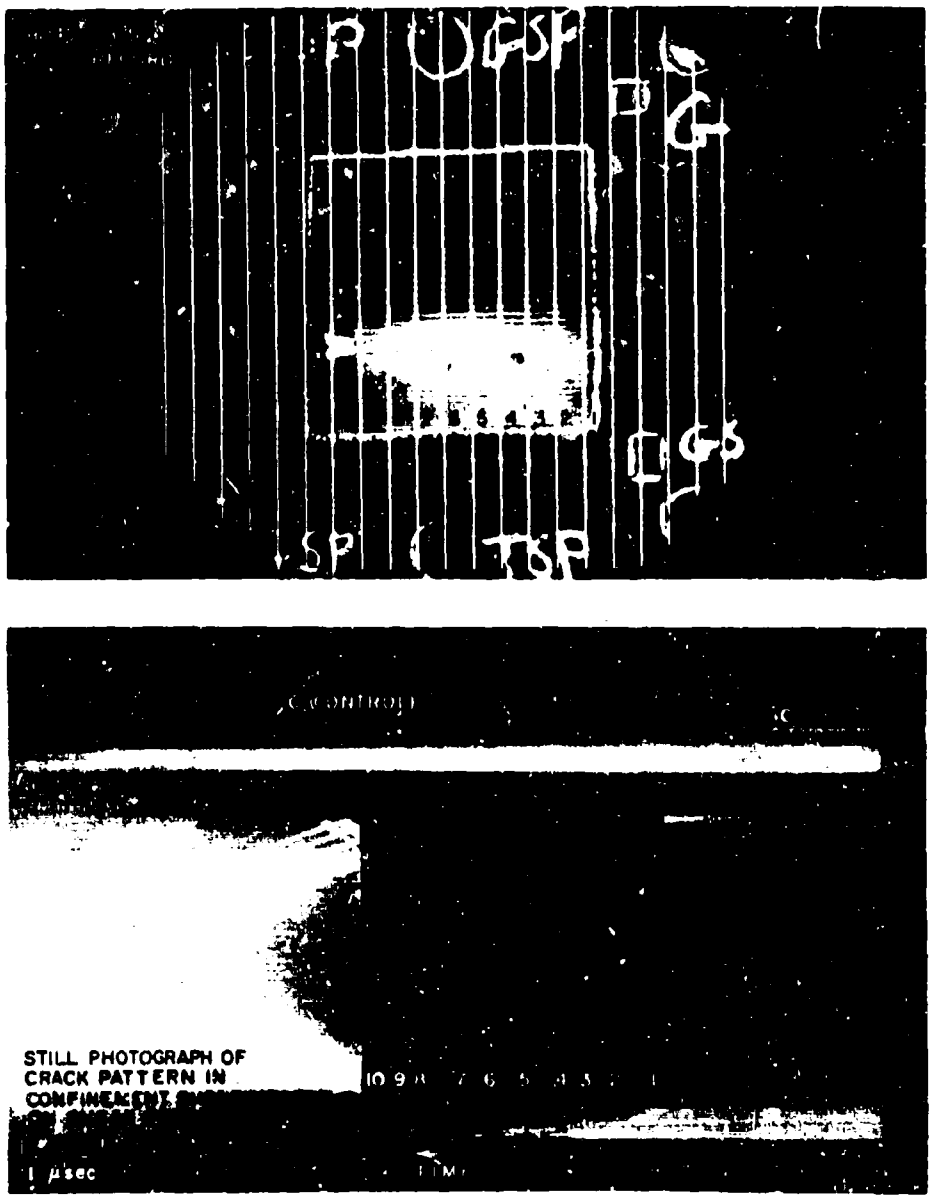

Figure 16 HEMICYLINDRICAL SHOT (30-mm Radius of Curvature)

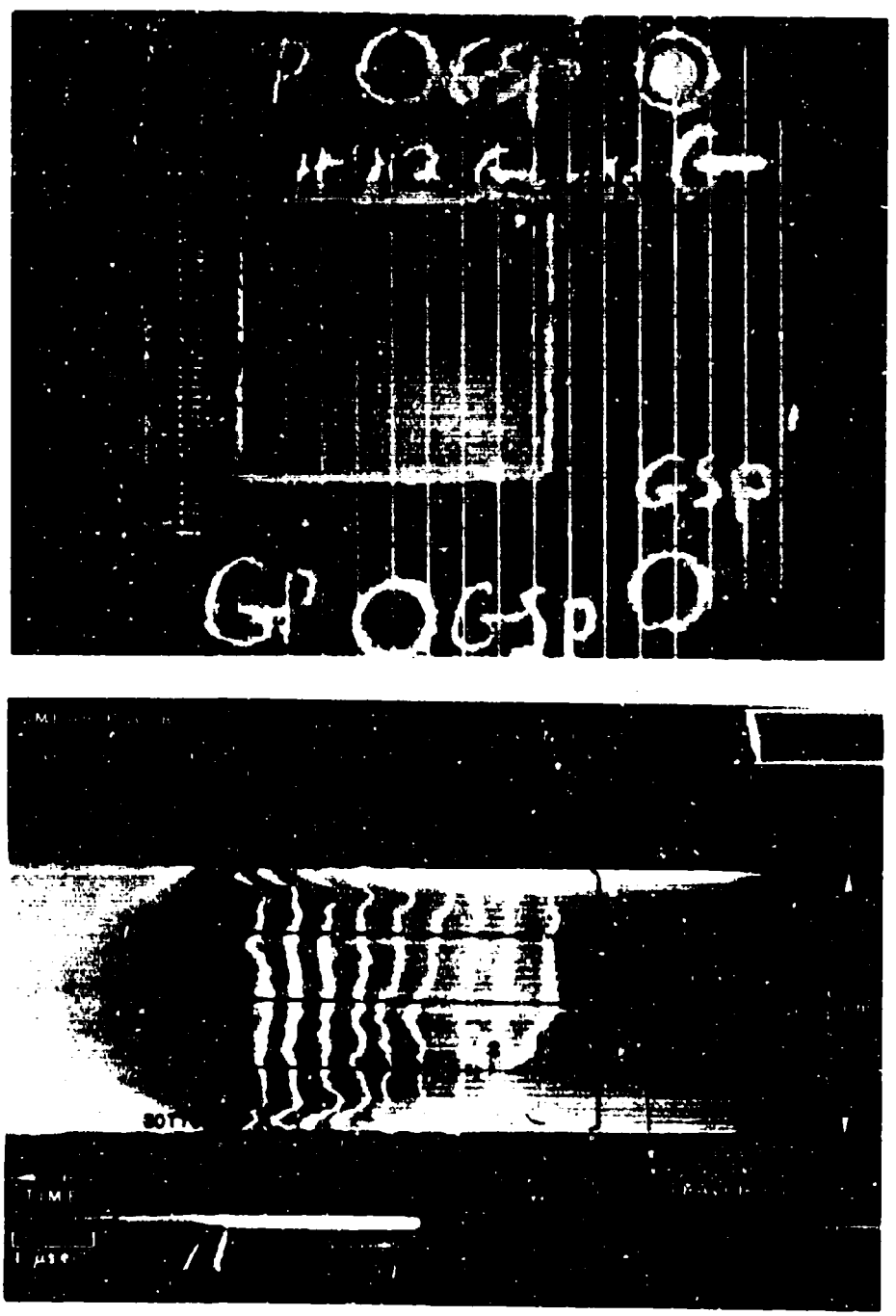

Figure 17 HEMICYLINDRICAL SHOT (25-mm Radius of Curvature)

h. Initiation of other explosives

The procedures used in attempting to initiate nitroglycerin or PETN by an argon flash were described in Sec. II-2g. In retrospect it seems that more Nigrosine black dye should have been dissolved in the nitroglycerin to make it more absorbent. Three readable records were obtained in six trials contained in a single shot. For all three the light "signal" emerging from the face opposite to that irradiated by the flash was diffuse and lasted for several microseconds. This is the type of signal one might associate with a deflagration rather than a detonation. The first discernible appearance of diffuse signals (these include transit times from the irradiated face to the camera face) occurred in 8.75 μsec for a quartz window assembly and 9.60 and ~14 μsec for glass window assemblies. Shock arrival at irradiated surfaces occurred in about 26 μsec. Clearly, some light-induced effect was thus observed. However, this effect is slow and variable and does not appear to produce a detonation in nitroglycerin columns about 1/4 inch in diameter and about 0.1 inch long.

In most trials with finely divided PETN, pure or mixed with fine graphite, the observed light signals corresponded to detonations. However, the time to the start of these signals always occurred after the shock in argon had arrived at the irradiated PETN surface. As shown in Table 10, the difference in time between shock arrival and start of light signal appears to be independent of window transmissivity--initiation occurred even with windows painted black. This delay also appears to be independent of PETN packing density. It may be a little longer for the PETN/graphite mixtures than for pure PETN and it definitely increases with increasing window thickness. Clearly, this is a shock initiation phenomenon and because it may be of some general interest, further discussion is presented in Appendix A.

Occasionally deflagration-like signals were observed with granular PETN prior to--and, less frequently, instead of--the detonation signals. These hard-to-read records are summarized in Table 11. The delay from start of flash to first discernible "deflagration" seems to depend in some

Table 10

ARGON SHOCK INITIATION OF GRANULAR PETN

SUMMARY

Type	Confinement	Density Range (g/cc)	No. of Obs.	Average Delay* (μsec)	Range (μsec)
PETN	1.5-mm quartz	0.72-1.54	8	2.09(a)	1.98-2.21(a)
PETN	1.0-mm glass	0.75	1	1.78	-
PETN	1.0-mm glass(b)	0.75-1.10	3	2.01	1.84-2.15
85/15 PETN/graphite	1.5-mm quartz	0.84-1.13	6	2.17	1.95-2.46
85/15 PETN/graphite	1.0-mm glass	0.85-1.01	3	2.06	1.91-2.25
85/15 PETN/graphite	0.1-mm FEP	0.86-0.88	2	1.35	1.33-1.37
90/10 PETN/graphite	1.0-mm glass	1.46	1	~2.2	-

* After shock strikes PETN surface; assuming that all the PETN detonates at a steady velocity controlled by its packing density.

(a) Omitting values of 1.49 and 1.75 μsec.

(b) Painted black - no absorbed argon shock radiation.

complicated fashion on energy and confinement. Generally delays are shorter with quartz windows than with glass. The more absorbent graphited PETN may give shorter delays with comparable windows than pure PETN (note last entry in Table 11 which contradicts this generalization). The single result with a Teflon FEP window, which transmits u.v. nearly as well as quartz, shows a long delay. This may indicate the need for heavier confinement. Even this initiation, which occurred about 2.2 μsec after the argon shock arrived at the irradiated surface, could have started before shock arrival since the transit time through the deflagrating PETN could easily have been much longer than 2.2 μsec (for a steady detonation established instantaneously at the irradiated surface the transit time would be 1.2 μsec).

Table 11

LIGHT "INITIATION" OF GRANULAR PETN

Type	Confinement	PETN Column		Total* Delay (μsec)	Shock Arrival (μsec)	Shot No.
		Height (mils)	Density (g/cc)			
90/10 PETN/graphite	1.5-mm quartz	100	1.43	12.5(a)	26.1	9,252
85/15 PETN/graphite	1.5-mm quartz	100	1.18	6.3	12.5	10,043
85/15 PETN/graphite	1.5-mm quartz	100	1.16	5.8	12.5	10,043
PETN	1.5-mm quartz	100	1.05	12.1	12.5	10,043
85/15 PETN/graphite	1.5-mm quartz	98	1.13	13.6	12.3	10,053
85/15 PETN/graphite	1.0-mm glass	100	1.01	14.0	12.3	10,053
85/15 PETN/graphite	1.0-mm glass	100	0.91	13.3	12.3	10,053
85/15 PETN/graphite	0.1-mm Teflon	244	0.86	14.2(b)	12.0	10,053
85/15 PETN/graphite	1.5-mm quartz	100	0.99	5.5	12.4	10,053

* To start of a discernible light signal.

(a) 8-inch u.v. reflecting mirror box; all others 4-inch u.v. reflecting mirror boxes.

(b) If steady detonation starts immediately, transit time is 1.2 μsec.

SECTION III

DISCUSSION

1. Dependence of Initiation Delay on Energy Absorption

a. Model of initiation process

As before,[2] it will be convenient to describe qualitatively a model for the initiation process and then examine its quantitative consequences. New data suggest the need for some modification of the original model,[2] although that model appears to be correct under conditions of good front-surface confinement and relatively low lead azide packing densities.

(1) Assume that the argon radiation absorbed by the azide appears primarily as heat and is used to raise the temperature of the azide.

(2) Assume that there is no heat loss.

(3) Assume that for most of the observed initiation delay there is no thermal decomposition of the azide and consequently no self-heating.

(4) Assume that self-heating, i.e., thermal decomposition, once it starts, leads to thermal explosion and detonation in very short times, provided that decomposition takes place in a sufficiently thick azide layer.

(5) Assume that the primary energy transport mechanism to achieve critical reaction zone thickness in the azide is via hot product gas flow from already reacted regions. Under favorable conditions this energy transport can be very rapid; hence, compared with the observed initiation delays, energy transport times are very short.

(6) When conditions for inward gas flow are unfavorable, energy transport to achieve critical thickness is via penetration of flash-bomb radiation into the azide regions below the "front" surface. This is a slower process than (5).

A sketch of the expected surface temperature-time profile in figure 18 may help clarify the proposed model for conditions favoring (5). Here τ is the observed initiation delay, τ_c is the time to reach T_c above which self-heating takes over, Q and c_v are heat of reaction and specific heat

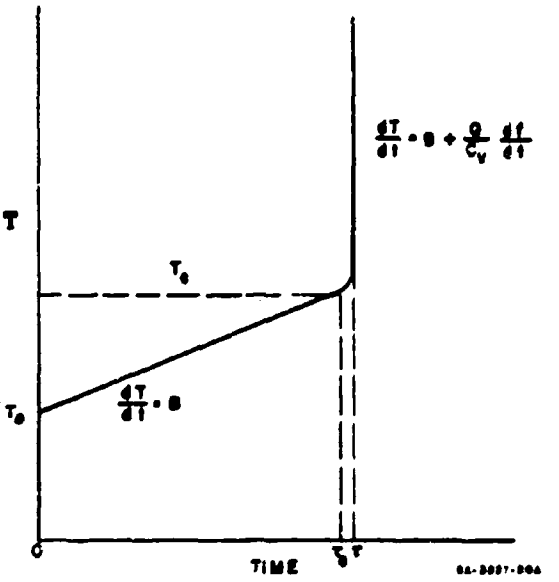

Figure 18 SKETCH OF THE POSTULATED TEMPERATURE-TIME PROFILE FOR THE INITIATION OF WELL-CONFINED, POROUS LEAD AZIDE

of lead azide, B is a constant, characteristic of the system used, and f is the fraction of azide decomposed in time, t.

Because τ is of the order of 1 to 10 μsec, and T_c has been shown[2] to be of the order of 900° K, assumption (2) appears to be sound; i.e., there is insufficient time for appreciable heat loss by conduction and T_c is too low for radiation to be important. Since chemical reaction rate is controlled by the term $\exp^{-E/RT}$, the abrupt change [assumption (3)] from no reaction to very rapid reaction seems reasonable, provided E, the activation energy of the rate-controlling process, is fairly large, as found.[2] Assumption (4) has been modified to bring in the realization that in order to establish a steady detonation a layer many molecules thick has to react in times comparable with τ or shorter. If the reacting layer is too thin, a rarefaction from the azide-confinement interface can quench reaction and prevent growth to detonation.

If the proposed model is correct, under favorable conditions of confinement and packing density, initiation occurs very shortly after any azide region of sufficient thickness reaches T_c, regardless of the window-filter system used. Thus it is to be expected that for these cases

$$T_c = \text{constant} = B\tau_c + T_o \sim B\tau + T_o$$

where B is the maximum rate of temperature rise of the lead azide. That T_c is constant, i.e., $B'\tau' + T'_o \sim B''\tau'' + T''_o$ has been established experimentally by measuring initiation delays for different window-filter combinations placed between the azide and the flash-bomb and also varying the ambient temperature.[2]

Consistent with assumption (2), heat conduction from the region of maximum reaction, located at essentially the mathematical front surface of the irradiated azide, is too slow to achieve temperatures of the order of T_c in times τ_c in a layer of the order of 1 μ thick. A posteriori justification for critical layer thicknesses of around 1 μ will be furnished later. Similarly, at any plane a distance x below the mathematical front surface,

radiation absorbed in time τ_c will raise the temperature by $B\tau_c e^{-\alpha x} < (T_c - T_o)$. Clearly under the usual conditions of good front-surface confinement and low packing density ($B\tau$ = constant) penetration of radiation cannot be the controlling mechanism by which a critical thickness is heated to around T_c. Under different conditions, namely, poor surface confinement or low porosity, penetration of argon radiation into the azide "interior" can become very important. For conditions under which $B\tau$ is constant, it is suggested* that the main process by which reaction is established in a critical thickness, is by hot gas flow from the reacted regions near the mathematical front surface. Figure 19 is a very rough schematic of what may be happening. Hot gas product clouds from irradiated regions of adjacent azide grains may interact with each other and with the front-surface confinement to form jet-like streams which impinge on the unirradiated portions of these grains and particularly the next layer of grains which are shadowed by the front layers. Hot gas is continually supplied from the reacting regions which now include not only the irradiated surfaces (which are likely to be molten lead azide just prior to appreciable reaction) but also areas heated to above T_c by the gas streams. This cumulative buildup of pressure and temperature could rapidly establish conditions required for steady detonation.

A previous attempt at explaining[7] the confinement effect is shown to be inapplicable in Appendix B.

b. New evidence for constancy of $B\tau$

A rigorous definition of B, the maximum rate of temperature rise of the lead azide, as given in Reference 7 is:

$$B = \frac{1}{c_v} \int_{\lambda_1}^{\lambda_2} \int_{o}^{\tau} A(\lambda)\, W(\lambda) \left[1 - R(\lambda)\right] \alpha(\lambda)\, I(\lambda, t)\, F(\lambda, t)\, dt\, d\lambda \qquad (4)$$

* The gas flow mechanism was suggested to the author by G. M. Muller of these Laboratories, who also designed figure 19, and set up the calculations discussed in Appendix B.

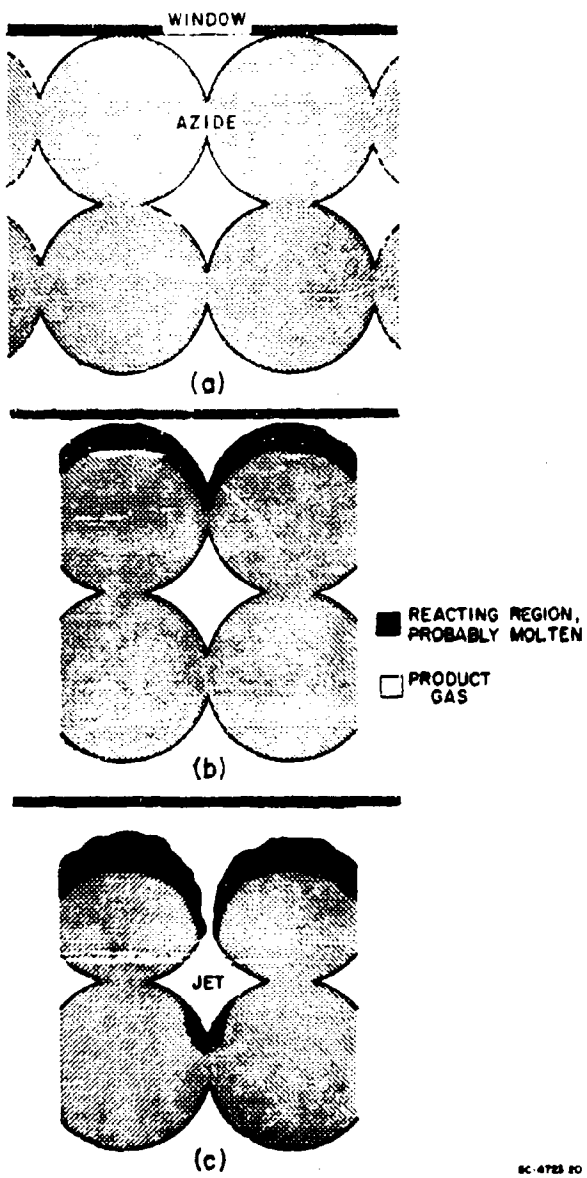

Figure 19 PROPOSED GAS FLOW MECHANISM: EFFECT OF CONFINEMENT (a) GRAIN CONFIGURATION BEFORE IRRADIATION, (b) EARLY REACTION STAGE, AND (c) JETTING AS THE RESULT OF INCREASING GAS PRESSURE. INITIATION OF REACTION AT SECONDARY SITES

where $W = \pi N$, N is the blackbody function of Eqs. (2) and (3), I is the relative light intensity, and F is a measure of the radiation divergence loss. The other symbols have the same meaning as those defined in figure 1. Figures 7 and 8 show that I changes quite slowly with λ and t for most of our experimental conditions. Consequently, it is sufficiently accurate to replace I by an effective light intensity $\bar{I}$ as defined by Eq. (1) and to take $\bar{I}$ outside the integral signs. Similarly, F is replaced by $\bar{F}_T$ as given by Eqs. (1), (11), and (12) of Reference 2. Equation (4) therefore is simplified to

$$B \sim \frac{\bar{F}_T \bar{I}}{\epsilon_v} \int_{\lambda_1}^{\lambda_2} A(\lambda) W(\lambda) [1 - R(\lambda)] \alpha(\lambda) \, d\lambda \qquad (5)$$

and the integral is evaluated numerically as before.[2]

It is reasonable to inquire whether $R(\lambda)$ and $\alpha(\lambda)$ measured at room temperature[2] remain unchanged as the azide gets hot. An affirmative answer is provided by the following experiments. Approximately 20-μ-thick disks of ball-milled PVA lead azide were placed on thin glass and irradiated through the glass by a "small-scale" (see Ref. 2) argon flash-bomb. The light transmitted through the window and disk was viewed with our photomultiplier system. The disk constitutes a very good diffuser and it is therefore to be expected that, if its characteristics do not change, the light transmitted increases as the radiating plane shock approaches the diffuser. As seen in figure 20, $\overline{FI}$ [$\bar{F}$ from the geometry of the system and Eq. (10), Ref. 2, and $\bar{I}$ from figure 7], which is a measure of the illumination of the azide disk by the advancing shock, is directly proportional to the observed light intensity transmitted through the disk. This could hardly be the case if either α or R changed appreciably as the azide temperature increased toward T_c. At the time τ, shown in figure 20, explosion presumably occurred and the transmissivity of the system decreased drastically because of chemical change and very much higher temperatures and/or shattering of the thin window. It is very gratifying that

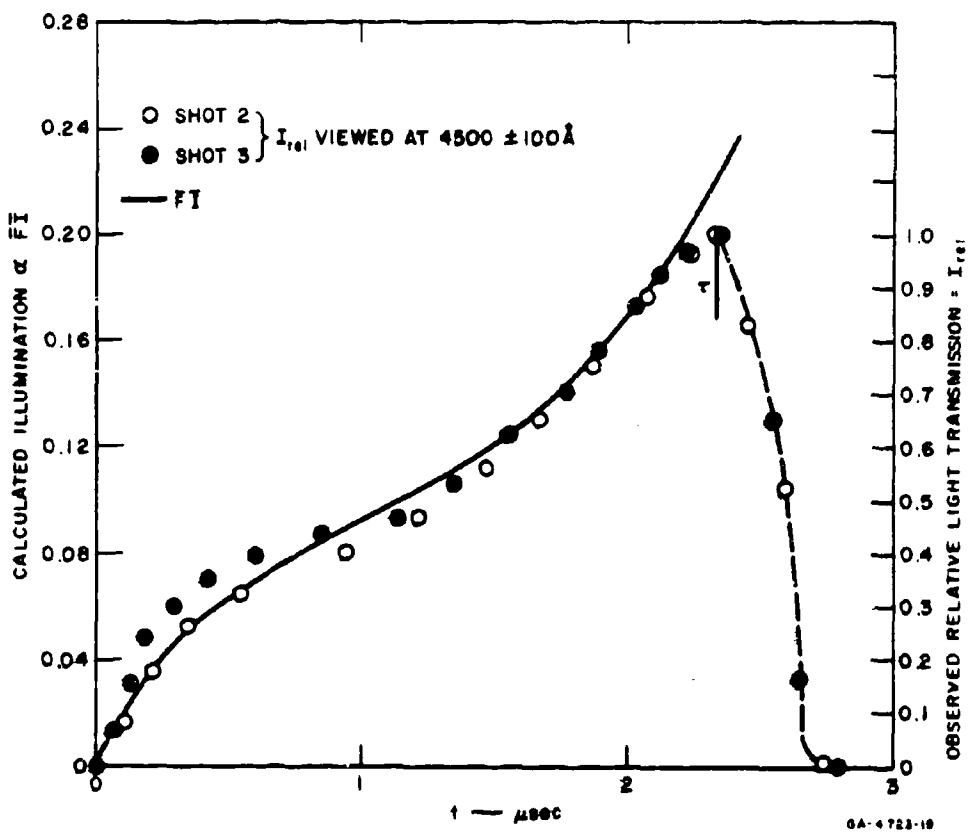

Figure 20 PROPORTIONALITY OF ILLUMINATION AND LIGHT TRANSMISSION OF THIN AZIDE DISKS

the $T_c = B\tau$, calculated on the basis of the τ of figure 20, is 590° K which is in excellent accord with the average T_c of 610° K (Table II, Ref. 7).

As already mentioned, it is to be expected that $B\tau$ = constant for low to intermediate azide packing densities and for good front-surface confinement. New results (those not reported in Ref. 2 or 7) are summarized in Table 12. Note that $B\tau$ is constant even for N_2 flash-bombs for which τ is about ten times longer than for argon flash-bombs. As indicated by the last entry in Table 12, as little as 1 mil of low-density plastic constitutes "good" front-surface confinement.

Table 12

CRITICAL TEMPERATURE RISE OF WELL-CONFINED, POROUS LEAD AZIDE AGGREGATES

Confinement	No. of Measurements	Normalized* Average Delay = $\bar{\tau}$ (μsec)	B_o** (°K/μsec)	B (°K/μsec)	$\Delta T_c = B\bar{\tau}$ (°K)
39-mil glass	many(a)	0.88	1300	693	610
29-mil glass	30	0.84	1390	715	610
39-mil glass	4	9.12(b)	111(b)	69(b)	620
29-mil glass	6	9.00(b)	117(b)	71(b)	645
65-mil quartz	2	6.40(b)	225(b)	92(b)	595
65-mil quartz	2	0.67(c)	~5000(c)	~860(c)	~575
29-mil glass	2	1.79(c)	1390(c)	330(c)	590
1-mil PVF	3	0.75	1840	800	600

* Maximum spread is around 0.1 $\bar{\tau}$ or less.

** Is the integral of Eq. (5) divided by c_v.

(a) See Reference 2.

(b) N_2 flash of T_{N_2} = 11,000° K; all others argon flash of T_A = 29,000° K.

(c) 4x4x4-inch "Black Box" - no reflections; all others mirror boxes, usually 4x4x8 inches.

It is seen from the last column of Table 9 that BT is not constant for sheet lead azide. All values are higher than the expected 610° K/μsec even after they have been corrected for an increase in τ due to the higher packing density of the sheet azide as compared with standard granular azide pellets. The values closest to the expected one are for Batch 7 sheet azide. There is reason to believe that this batch contains the least amount of Teflon binder. Batch 8 or Batch 13 which contain the largest amount of binder give the largest apparent BT. Consequently, the larger than expected BT's are understandable in terms of radiation absorption by the binder which, as is known from propellant technology, congregates on the sheet surfaces. The binder layers act as extra light filters.

c. Estimates of critical thickness

Figure 10 shows that as the porosity of well-confined azide aggregates is greatly reduced, initiation delay increases. At low packing density, moving the window away from the irradiated azide surface also increases initiation delay as shown in figure 21. Both these effects are understandable in terms of the critical reaction thickness model. If this model is correct, then under conditions which prevent gas flow into the interior and permit only penetration of radiation, for an observed delay τ',

$$T_c = \text{constant} = 610^\circ \text{ K} = B\tau' e^{-\bar{\alpha}\rho_o x} \qquad (6)$$

where $\bar{\alpha}$ is the average absorption coefficient (in cm^2/g) in a region x cm below the mathematical front surface of the azide. In words, Eq. (6) states that within a thickness x all the azide is at least as hot as the critical reaction temperature T_c. Since we are referring to individual grains, the appropriate density [ρ_o in Eq. (6)] is 4.8 g/cc, the crystal density of lead azide. Knowing τ' and B and estimating $\bar{\alpha}$ (from figure 10 and Table 12 of Ref. 2) one can solve for x. The results of these computations are summarized in Table 13. They lead to the following conclusions:

(1) At low packing density the calculated x increases with separation of azide and window. The big variation in x occurs between one mil and several mils separation. For larger separations, x does not change any further.

(2) The calculated x increases with packing density--rapidly at intermediate densities and very slowly at high densities.

(3) Over wide ranges (~250 to 1300° K/μsec) x is independent of B.

(4) Extrapolating the delay vs density plot for well-confined assemblies (figure 10) to crystal density and using this value in Eq. (6) gives $x \sim 1.1\,\mu$ which agrees very well with the critical thicknesses obtained at high densities in unconfined systems. This is strong evidence that the confinement effect and the density effect are caused by the same phenomena. This "measured" x justifies the use of ~1 μ critical thickness in Sec. III-1a.

(5) For very small B's (nitrogen flash) gas penetration somehow appears to be the main energy transport mechanism even under conditions where gas penetration has been largely eliminated at the higher rates of energy absorption. This apparent anomaly will be examined later.

Since steady detonation in homogeneous or heterogeneous materials is also believed[8] to be a thermal process, it may be suggested that the approximately 1-μ critical thickness found above is of the same magnitude as the reaction zone thickness in an established lead azide detonation. Certainly such a narrow reaction zone is consistent with the common observations of no diameter effect and no run-up to detonation for lead azide. The 1-μ critical thickness is also consistent with "hot spot" diameter estimates.[9]

Table 13

RAISED WINDOW EFFECT

Window	Separation* (mils)	Packing Density (g/cc)	Flash	No. of Obs.	$\bar{\tau}$ Normalized Avg Delay (μsec)	Range (μsec)	B (°K/μsec)	$\bar{\alpha}$ (cm^2/g)	x** (μ)
Glass	1	2.3 -2.4	Ar	4	1.41	1.37- 1.45	700	2.44	0.43
Glass	15-30	2.3 -2.4	↓	7	1.60	1.48- 1.70	700	2.44	0.53
Glass	15; vacuum	2.3 -2.4	↓	2	1.73	1.70- 1.77	700	2.44	0.61
None	∞	2.3 -2.4	Ar	21	0.96	0.89- 1.08	~1300	~2.7	~0.55
Glass(a)	8	3.7	Ar	2	1.73	1.71- 1.75	880	2.44	0.81
Glass(a)	9-13	4.13-4.16	↓	2	2.22	2.25- 2.19	910	2.44	1.02
Glass(a)	12	4.25	↓	1	2.21	-	910	2.44	1.01
Glass(a)	1(b)	2.36	Ar	2	2.91	2.89- 2.92	360	2.44	0.47
Glass	14(b)	2.36	↓	2	3.43	3.30- 3.58	370	2.44	0.64
Glass(a)	14(b)	4.12	↓	1	4.85	-	410	2.44	1.02
Glass(a)+0.3 ND	1	~2.4	Ar	2	3.58	3.57- 3.58	270	2.34	0.41
1-mil PVF	23		↓	2	1.25	1.22- 1.26	925	2.63	0.52
Glass(a)	1	2.38	N_2	2	9.63	9.31- 9.95	73	2.42	0.10
Glass(a)	30	2.46	↓	2	11.62	11.26-11.99	77	2.42	0.34
Glass(a)	8	~3.7	↓	1	11.69	-	77	2.42	0.34
Glass	0	4.8	Ar	-	~2.60(c)	-	840	2.44	1.07

* Between window and irradiated aside surface.

** From $B\bar{\tau}\exp(-\bar{\alpha}\rho_o x) = 610°K = \Delta T_c$; ρ_o = 4.8 g/cc - crystal density of PbN_6.

(a) 29-mil; others are 39-mil glass.

(b) 4-inch black box

(c) By extrapolation of Fig. 10..

d. Pressure rise during initiation

Figure 21 shows that the initiation delay in an unconfined system at an ambient pressure of 21 atm is considerably shorter than the delay in a similar system at 1 atm. It seems reasonable to expect a similar effect, regardless of how it is caused, from gas formed during the early stages of lead azide decomposition provided that this gas cannot escape too rapidly. For low pressures, i.e., early stages of decomposition, the gases produced should behave ideally and the pressure for a constant volume reaction will be given by

$$P = \frac{3\rho_o fT}{M} = KfT$$

where ρ_o is the packing density and M the molecular weight of lead azide, and f is the fraction of azide decomposed.

The product fT as a function of time and B can be obtained from numerical solutions of the heat balance equation [Eq. (18) of Ref. 2 or Eq. (5) of Ref. 7]. This was done for the following conditions:

$$E = 37\ \text{Kcal/mole},\quad Z = 10^{14}\ \text{sec}^{-1},\quad Q/c_v = 3250^\circ\text{K},\quad T_o = 300^\circ\text{K}.$$

The time differences between producing pressures of 10, 20, 40, and 100 atm and thermal explosion are given as functions of B, the energy absorption rate, in figure 22, which also shows some other information to be discussed later. These plots suggest that for low B, for which most of the decomposition occurs over a period of the order 0.1 μsec or more, the earliest stages of decomposition create an "ambient" pressure of several tens of atmospheres (for p = 40 atm, $f \sim 0.02$). Presumably such a pressure near the irradiated reacting surface is sufficient to deflect most of the subsequent hot gas product flow inward into the azide mass and create conditions favorable for the type of energy transport shown in figure 19. For most of the studied systems B is such that the duration of the intermediate pressure regime is so short that it could have less influence on the subsequent gas flow than in the case of a nitrogen flash of very low B.

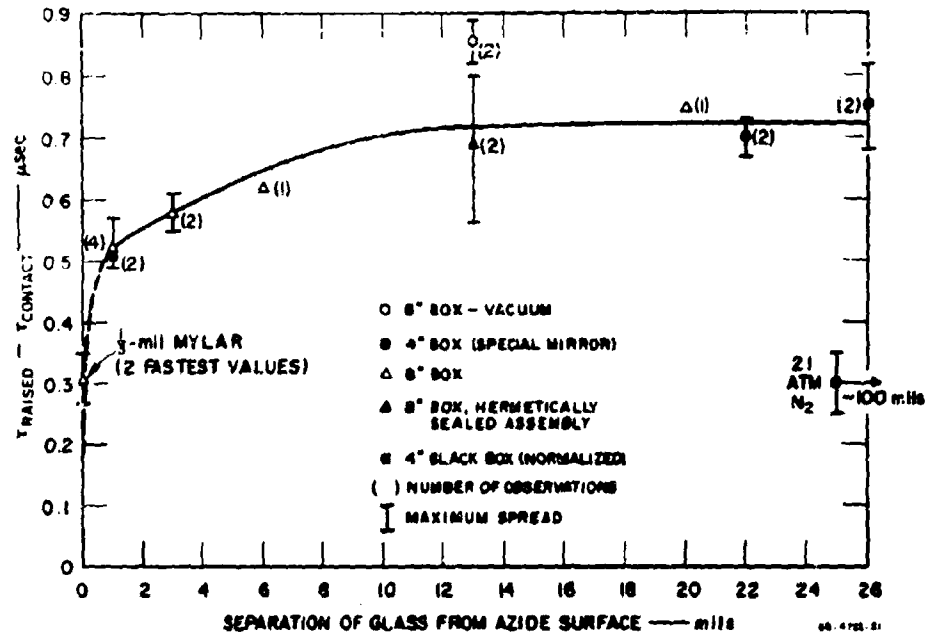

Figure 21 EFFECT OF INTIMACY OF FRONT-SURFACE CONFINEMENT ON INITIATION DELAY OF PVA LEAD AZIDE

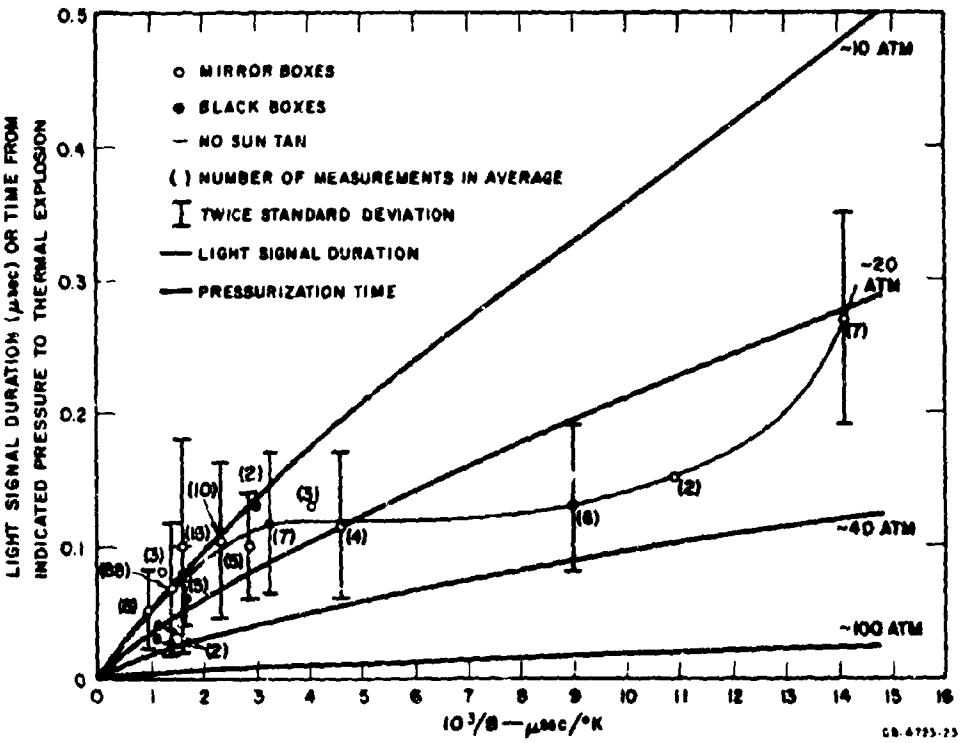

Figure 22 DURATION OF LIGHT SIGNALS FROM DETONATING LEAD AZIDE

However, the results in Table 13 (increase of x in vacuum and with separation of window) suggest that even for these high B systems there is some inward gas flow which is stopped only when the porosity of the system gets very low. It is also possible that high energy absorption rates create vigorous gas jets many of which escape from the irradiated surface if it is unconfined, and that this loss is less important at low B.

e. Types of light breakout

It has been pointed out that detonation starts very near (within ~1μ) the irradiated lead azide face but is viewed by the streak camera at the opposite face. Because of this it is not immediately apparent that the type of light signal recorded by the camera bears any relation to the conditions obtaining at the irradiated face. Considerable evidence has now been accumulated which shows that the system does have a "memory," so that conditions prevailing at the irradiated face do control the type of light signal observed. For instance, length or diameter of the azide column or sleeve material do not influence the type of signal produced but the rate of energy absorption does. Shielding the outermost periphery of the irradiated azide surface changes the type of signal and so does the intimacy of front-surface confinement.

The varieties of breakout signals have been classified into six groups which are sketched in the footnotes of Table 14. The frequency of occurrence of each of these groups for well-confined lead azide aggregates is shown in Table 14 as a function of B, the rate of energy absorption by the azide. Although there is variation and overlap, the trend is unmistakable. As B decreases the signals change from "symmetric" to "center" to "top or bottom." The latter type is also characteristic of poor confinement and possibly of high packing density. Symmetric signals must arise from uniform initiation all around the outer azide column periphery as sketched in figure 8 of Ref. 1. Not shown in the sketch are the multipoint initiations which must occur all over the irradiated surface a little later. These spherical wavelets coalesce to form a nearly plane wave front which

Table 14

TYPES OF LIGHT BREAKOUT SIGNALS*

Window Confinement	Filter	Density (g/cc)	B (°K/μsec)	Spectral Region	No. of Obs.	Frequency of Occurrence**					
						Symm.	Unsymm.	Near Straight	Center	Multiple	Top or Bottom
Quartz	None	2.3-2.4	~1050 - ~1100	u.v. and vis.	12	0.75	0.08	0.17	-	-	-
Quartz(a)	↓	2.14	660	↓	2	-	0.50	0.50	-	-	-
Quartz(a)	~2.3	350			2	-	-	-	0.50	0.50	-
None	2.3-2.4	~1300			21	0.67	-	-	0.06	0.23	0.06
7-54(a)	~2.3	900			2	-	-	0.50	-	0.50	-
7-54(a)	~2.3	490			2	-	-	-	0.50	0.50	-
PVF	2.3-2.4	775		↓	3	-	0.67	0.33	-	-	-
Glass(b)	None	2.2-2.4	700 - 835	near u.v. and vis.	110	0.19	0.12	0.46	0.09	0.03	0.11
Glass(b, a)	↓	~2.3	600	↓	6	-	-	0.33	0.50	0.17	-
Glass(b, a)	~2.3	300			3	-	-	-	0.67	0.33	-
Glass(b, a)	~2.3	160			6	-	0.33	0.17	0.17	0.17	0.17
Glass(b)	0.1 N.D.	~2.3	690		8	0.25	-	0.25	0.25	0.12	0.13
Glass(b)	0.2 N.D.	~2.3	350		5	-	0.20	-	0.60	0.20	-
Glass(b)	0.3 N.D.	~2.3	260		14	0.14	0.29	-	0.36	0.07	0.14
Glass(d)	None(c)	~2.3	700		5	-	-	0.20	0.80	-	-
Glass(d)	None	2.3-2.4	~790	↓	13	0.08	-	0.23	0.23	0.08	0.38
Glass(e)	None	~2.3	610 - 720	vis.	14	0.36	0.07	0.07	0.21	0.14	0.14
Glass(b)	0-52	~2.3	660	↓	11	-	0.18	0.18	0.64	0.09	0.09
Glass(b)	1A	~2.3	220		6	-	0.17	0.17	0.33	0.17	0.17
Glass(b)	7-54	~2.3	390	near u.v.	14	-	0.14	-	0.28	0.21	0.36
Glass(b, f)	None	2.3-2.4	580	near u.v. and vis.	12	0.08	0.50	0.17	-	-	0.25
Glass(e, f, f', k)	↓	~2.3	480	vis.	4	0.75	-	0.25	-	-	-
Glass(e, f)	~2.3	480	vis.	9	0.22	0.11	0.11	0.11	-	0.44	
Glass(b, g)	None	2.3-2.4	68 - 73	near u.v. and vis.	12	-	-	-	0.25	0.08	0.67
Quartz(g)	None	2.60	91	u.v. and vis.	2	-	-	-	-	1.00	-
Glass(b, h)	None	2.0-2.3	830	near u.v. and vis.	2	0.50	-	0.50	-	-	-
Glass(b, h, i)	↓	2.0-2.4	830	↓	3	-	0.33	0.33	0.33	-	-
Glass(b, h, i, j)	~2.4	830			2	-	-	-	-	-	1.00
Glass(b, h, i)	2.7	830			2	-	-	0.50	0.50	-	-
Glass(b, h, i, j)	2.7-3.0	830			2	-	-	-	-	-	1.00
PVF(h)	Glass(b)	3.10	575		2	-	1.00	-	-	-	-
PVF(h)	↓	3.00	590		1	-	-	-	-	-	1.00
PVF(h)	4.1-4.4	600	↓	2	-	-	0.50	-	0.50	-	
(PVF(a, h)	4.3	500		1	-	-	-	-	-	1.00	
Glass(b, j)	None	2.3-2.4	700	near u.v. and vis.	22	0.14	0.32	0.14	0.23	0.05	0.27
None(k)	Glass(b, h)	2.3-2.4	77 - 830	near u.v. and vis.	14	-	-	0.14	0.57	0.29	-
None	Glass(b, l)	2.3-2.4	77 - 700	↓	18	0.33	0.11	-	0.22	0.17	0.17
None	Glass(b, l)	2.7-4.3	77 - 830		9	-	-	-	0.11	0.22	0.67
Glass(b, m)	None	~2.5	~700	near u.v. and vis.	50	0.24	0.10	0.10	0.24	0.20	0.10

* From face opposite to that irradiated

** For time increasing →

Symmetric •

Unsymmetric • ⟩ or ⟩

Near Straight • —

Center • (

Multiple • }

Top • /

Bottom • \

(a) Black box - no reflected radiation.
(b) 39-mil or 29-mil glass; latter has slightly greater B.
(c) Approximately 1/16-inch-wide black tape placed around aside column periphery.
(d) Irradiated face tilted 15 to 60° from vertical
(e) 60-mil crown glass.
(f) "Pale" aside. All others "sun tanned."
(f') Aside is preheated 140 to 220°C.
(g) N_2 flush.
(h) Aside packed into metal sleeves; all others in nylon.
(i) Confinement attached to loaded sleeves.
(j) Poor confinement because of glue and/or aside between sleeve top surface and window.
(k) Window separated from aside by 1 mil of air.
(l) Window separated from aside by 5 to 30 mils of air.
(m) "Coarse" aside 5 to 20μ; all others about 0.5μ.

flattens the final portion of the light signal as shown in the footnotes of Table 14.

On the average the symmetric signal has a duration of around 0.05 μsec. Using this time in a simple model like the one in figure 8 of Ref. 1 leads to an azide detonation velocity which is much too high. Modifying this model, as suggested above, to include multipoint initiation, delayed some 0.05 μsec behind the peripheral initiation, leads to detonation velocities in good agreement with measurements by other techniques (see figure 2). The "unsymmetric" signals must also result from peripheral initiation but initiation which is no longer uniform in time. For unknown reasons these signals are generally "sharp" as shown and do not have the flattened portions of the symmetric signals. The "straight" signals quite obviously have their origin in nearly uniform initiation all over the surface. Because the azide face toward the camera is viewed by a single slit across it (see the still record of figure 13), very little can be said about the origins of the other type of signals except that they are nonuniform over the time scale of the order of 0.1 μsec.

Once again a reasonable explanation of the above observations is provided by the critical thickness model. For reasonably good front-surface confinement and intermediate azide packing density, energy transport to achieve critical thickness is believed to be primarily via product gas flow. One might expect that at high rates of energy absorption by the azide, product gas interactions, i.e., formation of inward flowing gas jets, is facilitated because gas pressures increase rapidly even in the early stages of decomposition at the irradiated surface. Conversely, when B is small, early decomposition is relatively slow, the gas streams are relatively "diffuse," and establishment of inward gas flow should be slower than above.

These considerations may explain the shift from "straight" signals to "top or bottom" signals as B decreases. The causes behind the preponderance of "symmetric" signals at the highest observed B's are not

understood except that in a general way one might expect optimum conditions for jet formation at the azide-sleeve-window interface.

It is fruitful to examine the total time duration of the lead azide light signals in terms of the critical thickness model. Figure 22 shows light signal duration of well-confined porous lead azide assemblies as a function of B as well as the pressurization time discussed in the previous section. Note the rather close correspondence between signal duration and the 10-atm pressurization at high B levels. As B decreases the signal duration curve tends toward pressurization curves of more than 10 atm--for example, toward 20 atm. In these assemblies $B\tau$ = constant (τ is taken to the start of the light signal), i.e., detonation is established very shortly after the thermal explosion of the foremost lead azide regions because energy transport to achieve critical thickness is very rapid. The finite duration of the light signal is presumably caused by small differences in time to achieve critical thickness for different regions of the decomposing azide. These differences depend on local circumstances but, since it is expected that these circumstances are generally randomly distributed over the entire azide face, the average signal duration should be of some significance. It is obvious that only a rather small portion of any azide grain is in true contact with the front-surface confinement (see figure 19). The model suggests that critical thickness resulting in detonation is first achieved near sites of true contact with the confinement because of favorable conditions for inward gas flow. In the more numerous "near-contact" regions initial gas flow is supposedly largely toward the confinement. These initial gas streams are reflected back into the azide by the confinement. Additionally, the air space of the near-contact regions becomes pressurized by the product gas and this also helps inward flow by minimizing the escape of subsequently formed gas. One might therefore expect a correspondence between signal duration (really the time difference between local establishment of detonation under favorable and somewhat less favorable local conditions) and the duration of the reaction-produced intermediate pressure regime. Large B, as already mentioned,

may aid the establishment of jet-like flow. Also, radiation penetration into the azide interior contributes appreciably to the energy transport. Consequently, it might be expected that for well-confined systems a lower level of self-pressurization is required at large B's than at lower ones. This may not be the case in unconfined systems for which the jet-like gas flow may contribute more toward escape rather than inward flow (see Sec. III-1d).

f. Liquid confinement

Before the importance of critical thickness was realized, it appeared that a transparent liquid could be the perfect confining medium since it would conform to the azide surface and fill in any irregularities. Glycerin and Kel-F oil were tried as confining liquids in a system very similar to that described for vacuum shots in Sec. II-2e. Instead of evacuation, the space between azide sheet and a glass retaining wall was filled with liquid. In three separate shots containing twelve liquid-confined assemblies it was found that these delays were much longer and much more variable than for the standard glass-confined assemblies. Obviously, the liquid filled most of the pores between azide grains and prevented energy transport via inward gas flow.

2. Surface Initiation

a. General considerations

It is clear that the ideas developed in the last few sections are as applicable to the surface initiation of lead azide sheet as they are to the initiation of small granular lead azide pellets. As above, jitter is primarily caused by variation in the intimacy of contact between the confinement and the azide sheet. The main role of the confinement is believed to be as reflector of outward moving gas products. Although not conclusively proved, it is believed that the slightly smaller observed jitter with glass confinement rather than plastic confinement (see Table 9) is caused by better contact, because of better glue-bonding, between azide and glass than between azide and plastic. It appears that the inherent variability of

the sheet azide is much less than the variability caused by varying confinement. The inherent variability (Batch 8 shows this more than any other) is presumably caused by variation in binder content and particularly by binder content at the surface. As already mentioned, a high binder content at the surface acts like an extra light-filter, thus decreasing the energy absorbed by the azide.

b. Recommendations for better sheet azide

It is expected that a binder which is easier to glue and more transparent than the presently used Teflon will greatly reduce azide sheet jitter. The azide content of a sheet with this sort of binder probably can be reduced below the present 95% level. At high packing density (low porosity) small changes in density result in large changes in initiation delay as shown in figure 10. Consequently it is desirable to keep azide sheet packing density fairly low--possibly a little lower than the present 2.5 to 2.7 g/cc. The presently attained sheet thickness tolerance of around 1 mil appears to be acceptable.

c. Applications

It is expected that the proposed surface initiation method will find its greatest usefulness in the study of the response of aerodynamic structures to simultaneous loading. To be applicable, this method must be capable of providing impulses in the useful range (typically 10^3 to 10^6 dynes sec/cm^2) with a simultaneity approaching 0.1 μsec. Impulse will be largely controlled by sheet thickness and confinement. The presently available sheets are 20 to 30 mils thick. These would provide impulses in the 10^5 to 10^6 dyne-sec/cm^2 range. In principle, there is no reason why the sheet cannot be made much thinner to reduce impulse. We have observed what appeared to be a detonation with 20-μ-thick granular azide disks (figure 20). It is known (Table 9) that 1-mil-thick plastic confinement is reasonably effective. It is believed that this effectiveness can be greatly improved by better gluing. Such thin low-density confinement should have little effect on impulse. The smallest jitters now obtained, if edge effects are

disregarded, are 0.2 to 0.3 μsec. We are convinced that better bonding of the azide sheet to its confinement can reduce this appreciably.

To control the loading of the test structure by the light-initiated lead azide, it is necessary to prevent the shock and explosive products of the light source from reaching the test structure. This can be done with mirrors as was done in the pumping of lasers by an explosive light source.[10] The main foreseeable limitation for such a system is that uniform illumination is limited to an area of a few square inches unless very large parabolic mirrors are used. It may be possible to keep a lower level of illumination over larger areas fairly uniform by using neutral density filters. A truncated pyramid made of mirrors was used in an attempt to spread the light from a small source to a larger area. As shown in Table 5, this was not too successful: jitter was rather large, since the central portions in this arrangement receive more radiation than the outer regions. It is believed that even without further improvements the "simultaneous" loading of a few square inches of a curved test structure can provide interesting information in a heretofore experimentally inaccessible area.

3. Future Work

Future efforts at improving the simultaneity of the proposed surface initiation system should be a part of a program of testing the response of small aerodynamic structures to simultaneous loads. It is believed that the main objectives of any such program should be (1) the improvement of contact between azide sheet and confinement, and (2) obtaining sheets of different thickness to provide a wider range in the available impulses. Both will require close coordination with the sheet supplier. The present supplier is rather inflexible and it would be most desirable to develop alternative sources of supply. Obviously, any test structure program will include the development of "remote" light sources and the determination of impulse constants for lead azide sheet.

APPENDIX A

SHOCK INITIATION OF PETN

This page intentionally left blank.

APPENDIX A

SHOCK INITIATION OF PETN

As shown in Sec. II-3h, our attempts to initiate PETN by radiation from an argon flash-bomb were unsuccessful. The detonations observed were caused by shock and/or flash-bomb detonation products. From the point of view of a shock-initiation experiment--of course our system was not designed to be a shock-initiation experiment--the analysis of a system consisting of flash-bomb explosive-argon-window-PETN is very complex. A crude and uncertain analysis by the method or characteristics,[11] using the pressure-particle velocity data of Seay and Seely[12] for PETN at 1 g/cc packing density and the results of Reynolds and Seely[13] for argon, leads to the following incident shock pressures in the PETN: quartz or glass windows, ≈0.5 kbar, FEP windows, ≈2 kbar; and no window, ≈5 kbar.

If one considers the quartz or glass windows as rigid walls and the argon as a perfect monatomic gas, then the approximately 1-kbar pressure in the argon shock[12] induces a 6-kbar pressure in the window.[14] Further, if one assumes the acoustic impedance match equation to be valid, then the pressure of the incident shock in PETN is ≈0.7 kbar, which is of the same order of magnitude as estimated above. Incident shock pressures of less than 1 kbar would not be expected to initiate detonation in PETN.[12] The 2-kbar shock estimated for the FEP window system also appears to be somewhat below the threshold of 2.5 kbar suggested in Ref. 12. It may be that the FEP windows are so thin (0.1 mm) that they provide no effective barrier between the argon shock and the PETN. The approximately 5 kbar obtained from the direct coupling of the argon shock to low-density PETN should be sufficient for initiating a detonation. In any event, the observed delays (Table 10) are appreciably less for these FEP windows than for the roughly equivalent delays in the thicker quartz or glass windows.

The two main questions posed by our observations (Table 10) are:
(1) Why do shocks of apparently less than 1 kbar initiate detonation in PETN?
(2) Why is the observed delay not increased by increasing PETN packing density? At this time only highly speculative answers can be provided. We have observed[2] that the plane shock in argon travels at a steady velocity for distances at least 10 to 20 cm from the original argon-flash-bomb explosive boundary. This would indicate that some of the detonation products of the explosive act as a constant velocity piston so that these products travel at the same velocity as the shocked argon particle velocity. If so, the detonation products would reach the neighborhood of the PETN pellets roughly 1/2 μsec behind the argon shock. The argon shock reflected from the PETN window will collide with the detonation products and a new and reinforced shock will be sent through the window into the PETN. Thus shortly after the initial shock of less than 1 kbar enters the PETN, a stronger shock is sent in. Presumably this second shock, or even later reverberations, can cause initiation. The absence of a packing density effect may be due to better acoustic coupling between the more dense PETN and the window, or perhaps the early reverberation pulses perturb the packing of the front PETN layers in which detonation is initiated.

APPENDIX B

THE EFFECT OF SURFACE CONFINEMENT

This page intentionally left blank.

APPENDIX B

THE EFFECT OF SURFACE CONFINEMENT

It is well established that the elapsed time, τ, between the beginning of the irradiation of the front surface of a lead azide pill and the emergence of a detonation wave from the rear face of the pill, is significantly shorter if the irradiated surface is confined by a thin glass, quartz, or plastic window than if the front surface is left bare. In any given shot with 40-mil-thick glass windows the difference in τ between the confined and unconfined cases is about 0.6 μsec. Effectiveness of confinement is independent of the material or thickness (down to 1 mil) of the window. There is, however, a strong dependence on the intimacy of contact between window and pill.

In trying to find an explanation for these observations, one is tempted to think first in terms of some form of heat loss at the bare front surface by which the onset of thermal explosion is retarded. Most of the more obvious mechanisms can be ruled out fairly easily. Heat conduction is too small and, in any case, works in the wrong direction since the window, being more transparent, would be expected to run cooler than the lead azide. Loss of heat from escaping reaction products is necessarily small prior to the occurrence of substantial reaction; moreover, the escaping nitrogen molecules having made on the average quite a few collisions within the bulk of unreacted material, will leave the surface at a temperature which cannot be much higher than that of the remaining material.

One mechanism that at first seemed to offer some hope of explaining the confinement effect involves the diffusion of neutral N_3 radicals. In the usual kinetic scheme for the decomposition of lead azide,[7] it is assumed that the primary (endothermic) step is

$$N_3^- + h\nu \longrightarrow N_3 + e^- ;$$

the frequency of occurrence of this step is governed by the usual Arrhenius

law for PbN_6, followed by the exothermic second-order reaction. This step is

$$N_3 + N_3 \longrightarrow 3\,N_2 + Q.$$

The second step depends on a reasonable mobility of the neutral azide radicals; this mobility is made possible by the weakening of the lattice forces when the temperature of the azide reaches or exceeds the melting point. On the other hand, the mobility of the radicals also allows them to escape (by diffusion) from the surface, and this escape is impeded or prevented by the presence of the solid window.

In order to investigate this mechanism, a machine computation was set up for solving the coupled heat conduction diffusion equations. If the density of the radicals is denoted by ϕ, the conditions of confinement and no confinement correspond approximately (according to diffusion theory) to the boundary conditions $\partial\phi/\partial x = 0$ and $\phi = 0$ at the free surface. Even when the (somewhat arbitrary) constants entering into the diffusion equation were chosen to be unrealistically extreme in the direction of emphasizing the difference in delay between confined and unconfined cases, this difference came out to be only 0.06 μsec. It is fair to conclude that the diffusion mechanism is not responsible for the confinement effect.

REFERENCES

1 Roth, J., Final Report TR 61-59, Project 8800, Contract AF 29(601)-2844, August 1961.

2 Roth, J., Final Report TDR 63-49, Project No. 5776/577601, Contract AF 29(601)-5134, March 1963.

3 Bagley, C. H., Rev. Sci. Inst. 30, No. 2, 103 (1959).

4 Christian, R. H., R. E. Duff, and F. L. Yarger, J. Chem. Phys. 23, 2045 (1955).

5 Thouvenin, J., Les Ondes de Detonation, Colloques Internationaux Du Centre National De La Recherche Scientifique, 1961.

6 Roth, J., J. Appl. Phys. 35, 1429 (1964).

7 Roth, J., J. Chem. Phys. 41, 1929 (1964).

8 Campbell, A. W., W. C. Davis, and J. R. Travis, Phys. Fluids 4, 498 (1961).

9 Bowden, F. P. and A. D. Yoffe, "Initiation and Growth of Explosion in Liquids and Solids," p. 65, Cambridge Press, 1952.

10 Crosby, J. K. and R. C. Honey, Appl. Optics 2, 1339 (1963).

11 Walsh, J.M., M. H. Rice, R. G. McQueen, and F. L. Yarger, Phys. Rev. 108, 196 (1957).

12 Seay, G. E. and L. B. Seely, J. Appl. Phys. 32, 1092 (1961).

13 Reynolds, C. E. and L. B. Seely, Nature 199, 341 (1963).

14 Courant, R. and K. O. Friedrichs, "Supersonic Flow and Shock Waves," p. 154, Interscience Publishers, 1948.

Unclassified

Security Classification

DOCUMENT CONTROL DATA - R&D

(Security classification of title, body of abstract and index annotation must be entered when the overall report is classified)

1. ORIGINATING ACTIVITY (Corporate author) Stanford Research Institute Menlo Park, California	2a. REPORT SECURITY CLASSIFICATION Unclassified 2b. GROUP

3. REPORT TITLE

STUDY ON SURFACE INITIATION OF EXPLOSIVES

4. DESCRIPTIVE NOTES (Type of report and inclusive dates)

Final Report 22 October 1963 to 9 April 1965

5. AUTHOR(S) (Last name, first name, initial)

Roth, J.

6. REPORT DATE November 1966	7a. TOTAL NO. OF PAGES 90	7b. NO. OF REFS 14
8a. CONTRACT OR GRANT NO. AF29(601)-6263 b. PROJECT NO. 5710 c. Subtask No. 15.018 d.	9a. ORIGINATOR'S REPORT NUMBER(S) AFWL-TR-65-135 9b. OTHER REPORT NO(S) (Any other numbers that may be assigned this report) SRI Project GHU-4723	

10. AVAILABILITY/LIMITATION NOTICES This document is subject to special export controls and each transmittal to foreign nationals or foreign governments may be made only with prior approval of AFWL (WLRP), Kirtland AFB, N.M. 87117. Distribution of this document is limited because of the technology discussed.

11. SUPPLEMENTARY NOTES	12. SPONSORING MILITARY ACTIVITY Air Force Weapons Laboratory (WLRP) Kirtland Air Force Base, New Mexico 87117

13. ABSTRACT

In response to a conti-ued military demand for controlled explosive wave shaping, this study was undertaken to establish basic conditions and to demonstrate the feasibility of an explosive system capable of being initiated uniformly along its entire surface. This investigation is a continuation of those started under AFSWC Contracts AF29(601)-2844 and -5134. It has demonstrated that under favorable conditions the simultaneity of detonation of a system consisting of surface-confined lead azide sheet, initiated by the radiation from an argon flash-bomb, approaches 0.2 μsec for plane or for hemicylindrical geometry. It is believed that this simultaneity can be improved if techniques for bonding the azide sheet to its confinement are improved. Even without further improvement, the proposed system of surface initiation is capable of providing valuable information in the heretofore experimentally inaccessible region of "simultaneous" loading of curved structures.

DD FORM 1 JAN 64 1473

Unclassified

Security Classification

Unclassified
Security Classification

14 KEY WORDS	LINK A		LINK B		LINK C	
	ROLE	WT	ROLE	WT	ROLE	WT
Surface initiation Lead azide gas-flow mechanism						

INSTRUCTIONS

1. ORIGINATING ACTIVITY: Enter the name and address of the contractor, subcontractor, grantee, Department of Defense activity or other organization (corporate author) issuing the report.

2a. REPORT SECURITY CLASSIFICATION: Enter the overall security classification of the report. Indicate whether "Restricted Data" is included. Marking is to be in accordance with appropriate security regulations.

2b. GROUP: Automatic downgrading is specified in DoD Directive 5200.10 and Armed Forces Industrial Manual. Enter the group number. Also, when applicable, show that optional markings have been used for Group 3 and Group 4 as authorized.

3. REPORT TITLE: Enter the complete report title in all capital letters. Titles in all cases should be unclassified. If a meaningful title cannot be selected without classification, show title classification in all capitals in parenthesis immediately following the title.

4. DESCRIPTIVE NOTES: If appropriate, enter the type of report, e.g., interim, progress, summary, annual, or final. Give the inclusive dates when a specific reporting period is covered.

5. AUTHOR(S): Enter the name(s) of author(s) as shown on or in the report. Enter last name, first name, middle initial. If military, show rank and branch of service. The name of the principal author is an absolute minimum requirement.

6. REPORT DATE: Enter the date of the report as day, month, year, or month, year. If more than one date appears on the report, use date of publication.

7a. TOTAL NUMBER OF PAGES: The total page count should follow normal pagination procedures, i.e., enter the number of pages containing information.

7b. NUMBER OF REFERENCES: Enter the total number of references cited in the report.

8a. CONTRACT OR GRANT NUMBER: If appropriate, enter the applicable number of the contract or grant under which the report was written.

8b, 8c, & 8d. PROJECT NUMBER: Enter the appropriate military department identification, such as project number, subproject number, system numbers, task number, etc.

9a. ORIGINATOR'S REPORT NUMBER(S): Enter the official report number by which the document will be identified and controlled by the originating activity. This number must be unique to this report.

9b. OTHER REPORT NUMBER(S): If the report has been assigned any other report numbers (either by the originator or by the sponsor), also enter this number(s).

10. AVAILABILITY/LIMITATION NOTICES: Enter any limitations on further dissemination of the report, other than those imposed by security classification, using standard statements such as:

(1) "Qualified requesters may obtain copies of this report from DDC."

(2) "Foreign announcement and dissemination of this report by DDC is not authorized."

(3) "U. S. Government agencies may obtain copies of this report directly from DDC. Other qualified DDC users shall request through _____."

(4) "U. S. military agencies may obtain copies of this report directly from DDC. Other qualified users shall request through _____."

(5) "All distribution of this report is controlled. Qualified DDC users shall request through _____."

If the report has been furnished to the Office of Technical Services, Department of Commerce, for sale to the public, indicate this fact and enter the price, if known.

11. SUPPLEMENTARY NOTES: Use for additional explanatory notes.

12. SPONSORING MILITARY ACTIVITY: Enter the name of the departmental project office or laboratory sponsoring (paying for) the research and development. Include address.

13. ABSTRACT: Enter an abstract giving a brief and factual summary of the document indicative of the report, even though it may also appear elsewhere in the body of the technical report. If additional space is required, a continuation sheet shall be attached.

It is highly desirable that the abstract of classified reports be unclassified. Each paragraph of the abstract shall end with an indication of the military security classification of the information in the paragraph, represented as (TS), (S), (C), or (U).

There is no limitation on the length of the abstract. However, the suggested length is from 150 to 225 words.

14. KEY WORDS: Key words are technically meaningful terms or short phrases that characterize a report and may be used as index entries for cataloging the report. Key words must be selected so that no security classification is required. Identifiers, such as equipment model designation, trade name, military project code name, geographic location, may be used as key words but will be followed by an indication of technical context. The assignment of links, rules, and weights is optional.